

Heart-enriched long noncoding RNA NPPA-AS1 regulates pathological cardiac hypertrophy by initiating a EP300-GATA4 axis

chunyu zeng (✉ chunyuzeng@163.com)

The Third Military Medical University

Zaicheng Xu

Daping Hospital, The Third Military Medical University, Chongqing Institute of Cardiology

Cong Lan

Department of Cardiology, Daping Hospital, Third Military Medical University

Caiyu Chen

Daping Hospital, Third Military Medical University

Yang Yang

Daping Hospital, The Third Military Medical University, Chongqing Institute of Cardiology

Nian Cao

Third Military Medical University

Junyi Yu

The Third Military Medical University

Hao Luo

Daping Hospital, The Third Military Medical University, Chongqing Institute of Cardiology

Ken Chen

Department of Cardiology, The General Hospital of Western Theater Command <https://orcid.org/0000-0002-8958-1088>

Li Guo

The Third Military Medical University

Hongyong Wang

The Third Military Medical University

Qiao Liao

Third Military Medical University

Chuanwei Li

Daping Hospital, The Third Military Medical University, Chongqing Institute of Cardiology

Xue Gong

Zhi Chen

The Third Military Medical University

Jiahui Jiang

The Third Military Medical University

Dezhong Yang

Daping Hospital, Third Military Medical University

Da-zhi Wang

Department of Cardiology, Boston Children's Hospital, Harvard Medical School, Boston

Pedro A Jose

The George Washington University School of Medicine and Health Sciences <https://orcid.org/0000-0003-1507-7556>

Gengze Wu

Daping Hospital, Third Military Medical University

Article

Keywords: long noncoding RNA, cardiac hypertrophy, NPPA-AS1, EP300, GATA4, 27 CRISPR–Cas9, GapmeR

Posted Date: April 19th, 2022

DOI: <https://doi.org/10.21203/rs.3.rs-1505479/v1>

License:  This work is licensed under a Creative Commons Attribution 4.0 International License.

[Read Full License](#)

1 **Heart-enriched long noncoding RNA NPPA-AS1 regulates pathological cardiac**
2 **hypertrophy by initiating a EP300-GATA4 axis**

3
4 Zaicheng Xu^{1,2,10*}, Cong Lan^{1,2*}, Caiyu Chen^{1,2*}, Yang Yang^{1,2}, Nian Cao^{1,2}, Junyi Yu^{1,2}, Hao
5 Luo^{1,2}, Ken Chen^{1,2}, Li Guo³, Hongyong Wang^{1,2}, Qiao Liao^{1,2}, Chuanwei Li^{1,2}, Xue Gong^{1,2}, Zhi
6 Chen^{1,2}, Jiahui Jiang^{1,2}, Dezhong Yang^{1,2}, Da-zhi Wang⁴, Pedro A. Jose⁵, Gengze Wu^{1,2#}, Chunyu
7 Zeng^{1,2,6-9#}.

8
9 ¹Department of Cardiology, Daping Hospital, The Third Military Medical University;

10 ²Chongqing Key Laboratory for Hypertension Research, Chongqing Cardiovascular Clinical

11 Research Center, Chongqing Institute of Cardiology, Chongqing, P. R. China; ³Department of

12 Endocrinology, Southwest Hospital, Third Military Medical University, Chongqing, P.R. China;

13 ⁴Department of Cardiology, Boston Children's Hospital, Harvard Medical School, Boston;

14 ⁵Division of Renal Disease & Hypertension, The George Washington University School of

15 Medicine & Health Sciences, Washington, DC; ⁶State Key Laboratory of Trauma, Burns and

16 Combined Injury, Daping Hospital, The Third Military Medical University, Chongqing, P.R.

17 China. ⁷ Heart Center of Fujian Province, Union Hospital, Fujian Medical University, Fuzhou,

18 P.R. China. ⁸ Department of Cardiology, Chongqing General Hospital, Chongqing, P. R. China.

19 ⁹Cardiovascular Research Center of Chongqing College, Chinese Academy of Sciences,

20 University of Chinese Academy of Sciences, Chongqing, P. R. China. ¹⁰Department of Cancer

21 Center, Second Affiliated Hospital, Chongqing Medical University, Chongqing, China.

22
23
24
25
26 **#Correspondences:**

27 Chunyu Zeng, MD, PhD, FACC; E-mail: chunyuZeng01@163.com

28 Gengze Wu, MD, PhD; E-mail: wugengze@163.com

29

30

1 **Abstract**

2 **Aims:** Cardiac hypertrophy, in the long-term, is a maladaptive response to the change in
3 hemodynamics needed to maintain cardiac output that leads to heart failure and sudden death.
4 However, the underlying regulatory mechanisms causing cardiac hypertrophy remain to be
5 elucidated. Recent studies have highlighted the importance of long non-coding RNAs (lncRNAs)
6 in many biological processes and diseases. However, knowledge of the role of lncRNAs in cardiac
7 diseases is still limited.

8 **Methods and Results :** We identified the role of NPPA-AS1 in cardiac hypertrophy and
9 remodeling. NPPA-AS1 is a heart-enriched and -conserved lncRNA, located in the antisense
10 strand of the atrial natriuretic peptide (*NPPA*) gene. The cardiac expression of NPPA-AS1 was
11 markedly upregulated early and sustained, in response to stress caused by transverse aortic
12 constriction (TAC) in mice. NPPA-AS1 levels were also increased in failing human hearts. To
13 determine the functional role of NPPA-AS1 in the heart *in vivo*, we inactivated NPPA-AS1 in mice
14 using CRISPR-Cas9. Under basal conditions, there was no body or cardiac morphological or
15 functional phenotype in NPPA-AS1-inactivated mice. However, *in vivo* germline inactivation of
16 NPPA-AS1 minimized the TAC-induced cardiac hypertrophy and fibrosis and normalized the
17 cardiac size, weight, and function. GapmeR-mediated or AAV9-shRNA-mediated silencing of
18 NPPA-AS1 could also block and attenuate TAC-induced pathological cardiac remodeling, which
19 reveals its clinical translation potential. The beneficial cardiac effects of inhibition of NPPA-AS1
20 were related to the recruitment of transcriptional coactivator EP300 to bind with transcription
21 factor GATA4 to promote GATA4 acetylation and inhibition of hypertrophic gene expression.

22 **Conclusions:** Our studies show that NPPA-AS1 recruits the transcriptional factor GATA4,
23 increasing EP300/GATA4 binding and subsequent GATA4 acetylation to promote pathological
24 cardiac hypertrophy. Inhibition of NPPA-AS1 could serve as a potential therapeutic strategy in the
25 treatment of maladaptive cardiac hypertrophy and remodeling.

26 **Key Words:** long noncoding RNA; cardiac hypertrophy; NPPA-AS1; EP300; GATA4;
27 CRISPR-Cas9; GapmeR.

28

1 Introduction

2 Cardiac hypertrophy, in the long-term, becomes a maladaptive response to hemodynamic
3 changes to maintain normal cardiac output¹, leading to heart failure and sudden death^{2, 3}, which is
4 the end-stage pathological process of various heart diseases. Cardiac hypertrophy is characterized
5 by cell area increase and caused by reprogramming of the cardiomyocyte transcriptome, including
6 the regulation of fetal genes, such as brain natriuretic peptide (NPPB) and β myosin heavy chain
7 (MYH7)⁴⁻⁶. These processes lead to remodeling and eventually deterioration of cardiac function^{5,6}.
8 The current pharmacological treatments of cardiac hypertrophy and remodeling delay the
9 progression of the disease but the mortality still high⁷. Thus, there is a need for new preventive
10 and therapeutic targets.

11 Long noncoding RNAs (lncRNAs) are transcripts larger than 200 nucleotides, with no
12 potential for protein-coding⁸⁻¹⁰. There are several classes of lncRNAs based on its position and
13 orientation in the genome¹¹; they act as signals¹², decoys¹³, guides¹⁴, scaffolds¹⁵ and enhancers¹⁶.
14 Emerging evidence has shown that lncRNAs participate in various biological systems and multiple
15 networks regulating gene expression¹⁷ and play important roles in normal physiology and
16 metabolism and diseases¹⁸⁻²⁰. Recent studies have indicated that some lncRNAs play roles in
17 cardiovascular pathophysiology, including cardiac hypertrophy. For example, lincRNA-p21
18 represses smooth muscle cell proliferation and induces apoptosis²¹; LncRNA Braveheart (Bvht)²²
19 and Fendrr²³ can promote cardiac development; Myheart (Mhrt) sequesters Brg1 from its genomic
20 DNA targets to prevent chromatin remodeling, protecting the heart from pathological cardiac
21 hypertrophy²⁴. Chaer, an epigenetic checkpoint, can accelerate cardiac hypertrophy progress²⁵ and
22 Chast promotes cardiac remodeling by negatively regulating pleckstrin homology domain²⁶. The
23 function and related mechanisms by which lncRNAs regulate cardiac hypertrophy and remodeling
24 await further studies. In this report, we identify the role of NPPA-AS1 in cardiac hypertrophy and
25 remodeling. NPPA-AS1 regulates genes in the cardiac hypertrophy network. Inactivating
26 NPPA-AS1 expression reduces cardiac hypertrophy and remodeling, indicating that NPPA-AS1
27 could be a potential therapeutic target in the treatment of cardiovascular diseases²⁷.

28

1 Results

2 **NPPA-AS1 is a cardiac-enriched and hypertrophy-associated lncRNA**

3 To identify the dynamic transcriptome changes during cardiac hypertrophy, we performed a
4 microarray analysis in remodeling hearts induced by transverse aortic constriction (TAC) in mice
5 (**Figure 1A**). We first filtered for all lncRNAs whose expressions were consistently dysregulated
6 in hearts that were stressed by TAC for one and two weeks [fold-change (FC) > 1.2]. The top 6
7 upregulated transcripts were selected and validated by q-PCR. Among them, lncRNA NPPA-AS1
8 was markedly upregulated after one or two weeks of TAC (**Figure 1B**).

9 After analyzing its expression in different tissues, NPPA-AS1 was found to be abundant in
10 the hearts of mice and human (**Supplemental Figures 1A-1C**). To determine whether
11 dysregulated NPPA-AS1 expression is associated with human cardiac hypertrophy and remodeling,
12 we examined the expression of human NPPA-AS1 with digital PCR, using total RNAs isolated
13 from hearts of patients with cardiac failure. As expected from the studies in mice, the copy number
14 of NPPA-AS1 in the hearts of patients with failure were significantly higher compared with
15 control group (**Figure 1C**). The expression of coding gene NPPA was also increased in hearts of
16 patients with cardiac failure relative to normal hearts (**Figure 1D**). Interestingly, NPPA-AS1
17 expression was also increased in the serum from patients with hypertension and hypertensive
18 cardiac hypertrophy, as compared with normotensive controls (**Supplemental Figure 1D**). The
19 characteristics of patients and controls are listed in the **Supplemental Table 1**. NPPA-AS1 is in
20 the anti-sense strand of *NPPA*, the coding gene for atrial natriuretic peptide (NPPA) and has two
21 exons overlapping with *NPPA* and one exon overlapping with chloride voltage-gated channel 6
22 (*CLCN6*) (**Figure 1E**). Using 3' and 5' RACE experiments, we identified that NPPA-AS1 is a
23 single, 1758-nt transcript with three exons. Protein Coding Potential Calculator²⁸ (CPC,
24 http://cpc.cbi.pku.edu.cn/programs/run_cpc.jsp) and Coding Potential Assessment Tool²⁹ (CPAT,
25 <http://lilab.research.bcm.edu/cpat/>) suggested that NPPA-AS1 is a non-coding transcript
26 (**Supplemental Figures 1E and 1F**), with limited conservation among rodents and other species,
27 including human, by blasting in UCSC website (<https://genome.ucsc.edu/>) (**Supplemental Figure**
28 **1G**). NPPA-AS1 is highly expressed in the nucleus of cardiomyocytes, determined by
29 quantification of nuclear/cytoplasmic RNA assay and RNA fluorescence *in situ* hybridization
30 (FISH) (**Figures 1F-1G and Supplemental Figure 1H**). Furthermore, we found that NPPA-AS1
31 was up-regulated 6 hours after TAC and lasted for at least 6 weeks (**Figure 1H**), suggesting that
32 NPPA-AS1 may work in the process of cardiac remodeling in mice.

34 **Inactivating function sequence of NPPA-AS1 blocks cardiac hypertrophy *in vitro* and *in vivo***

35 To show direct evidence of NPPA-AS1 involvement in cardiac hypertrophy, we used loss-
36 and gain-of function approaches in neonatal rat ventricular myocytes (NRVMs). NPPA-AS1
37 knock-down by siRNA had no effect on cardiomyocyte morphology under basal conditions but it
38 significantly suppressed phenylephrine (PE)-induced cardiomyocyte hypertrophy, evidenced by
39 the abrogation of the stimulatory effect of PE on cell surface area (**Supplemental Figures 2A-2B**)
40 and expression of fetal genes including NPPB and MYH7 (**Supplemental Figure 2C**).
41 Overexpression of NPPA-AS1 increased cardiomyocyte size, and expressions of MYH7
42 (**Supplemental Figures 2D-2F**). Collectively, these *in vitro* data suggest that NPPA-AS1 is an
43 important regulator of cardiac hypertrophy.

1 The above-mentioned *in vitro* results suggest that NPPA-AS1 could accelerate cardiac
2 hypertrophy. To support this hypothesis *in vivo*, we used the CRISPR–Cas9 editing approach to
3 generate NPPA-AS1-inactivated mice (**Figure 2A**). And to avoid disturbing the transcription of
4 last exon of CLCN6 gene, a 3X poly adenylate tail was inserted into the genomic DNA locus after
5 the first exon of NPPA-AS1, to premature termination of the transcription of exons 2 and 3 of
6 NPPA-AS1, which leads to a truncated NPPA-AS1 transcript. As expected, based on the protocol,
7 the expression of exon 3 of NPPA-AS1 was decreased while expression of exon 1 was normal
8 (**Supplemental Figure 3A**). In the basal state, the NPPA-AS1-inactivated mice developed well,
9 with normal body weight, normal cardiac morphology and function, similarly to the wild-type
10 mice (**Supplemental Figures 3B-3E**). By contrast, TAC-induced cardiac hypertrophy, determined
11 by heart weight/body weight ratio and gross morphology, was significantly reduced in
12 NPPA-AS1-inactivated mice, as compared with wild-type mice subjected to TAC for 6 weeks
13 (**Figures 2B and 2C**). Histological analyses also showed that the TAC-induced increases in left
14 ventricular wall and interventricular septal thicknesses were blunted in NPPA-AS1-inactivated
15 mouse hearts (**Figure 2C**). Wheat germ agglutinin (WGA) staining found that inactivating
16 NPPA-AS1 substantially blocked the increase in cardiomyocyte size induced by TAC (**Figures 2C**
17 **and 2D**). In addition, the TAC-induced increase in cardiac fibrosis was substantially suppressed by
18 NPPA-AS1 inactivation (**Figures 2C and 2E**). The inhibition of cardiac hypertrophy by
19 NPPA-AS1 inactivation was of pathophysiological significance because the decreased cardiac
20 function, induced by TAC, was ameliorated by NPPA-AS1 inactivation (**Figure 2F**). The
21 reprogramming fetal genes, including NPPB and MYH7, induced by TAC, were markedly
22 suppressed by germline NPPA-AS1 inactivation (**Supplemental Figure 3F**). These results
23 indicate that NPPA-AS1 plays a key role in cardiac hypertrophy and remodeling.

24 Besides germline *in vivo* inactivation of NPPA-AS1 in mice, using the CRISPR–Cas9 method,
25 we also knocked down all three exons of NPPA-AS1 in newborn mice (1 day after birth) by the
26 intraperitoneal injection of adeno-associated virus serotype 9 (AAV9) vector, carrying NPPA-AS1
27 shRNA, as described previously³⁰ (**Supplemental Figures 4A and 4B**). Consistent with the results
28 in NPPA-AS1-inactivated mice, the mice with post-natal NPPA-AS1 silencing developed well,
29 with normal body weight, cardiac morphology and function (**Supplemental Figures 4C-4E**), and
30 significantly reduced TAC-induced cardiac hypertrophy, assessed by heart weight/body weight
31 ratio, cardiac morphology, cardiac fibrosis, fetal genes expressions and ameliorated the decreased
32 cardiac function (**Supplemental Figures 4E-4J**).

34 **GATA4 is the effector of NPPA-AS1 regulating cardiac hypertrophy**

35 To explore the down-stream genes regulated by NPPA-AS1 in cardiac hypertrophy, a global
36 mRNA microarray was performed for RNAs isolated from NRVMs. GO and KEGG pathway
37 analyses showed a broad effect of NPPA-AS1 on transcriptional reprogramming of networks that
38 control cardiac hypertrophy and remodeling, including cell proliferation and growth, apoptosis,
39 inflammatory response, hypertrophic cardiomyopathy, and dilated cardiomyopathy
40 (**Supplemental Figure 5**).

41 As a nuclear lncRNA, that could regulate clusters of genes transcription, we wondered
42 whether NPPA-AS1 plays a role in pathological cardiac hypertrophy by specifically binding with
43 cardiac remodeling-related transcription factors to regulate target genes transcription. To verify
44 this hypothesis, we selected cardiac hypertrophy and remodeling related transcription factors, to

1 build a candidate pool, followed by computational prediction and experimental validation using
2 chromatin isolation by RNA purification (ChIRP) assays (**Figure 3A**). catRAPID, a predictor of
3 protein-RNA binding³³ (http://big.crg.cat/gene_function_and_evolution/services/catrapid),
4 predicted NPPA-AS1 might interact with GATA4, GATA6, MEF2C, NKX2-5, FOXO3A, and
5 HIF1A (**Figure 3B** and **Supplemental Figure 6A**). Furthermore, ChIRP and RNA Binding
6 Protein Immunoprecipitation (RIP) assays showed that only GATA4 could bind with NPPA-AS1
7 (**Figures 3C-3D** and **Supplemental Figure 6B**). catRAPID predicted that NPPA-AS1 might bind
8 with RNA binding protein (RBPs) through nucleotides (nt) 1400 to 1600 and 100 to 200 (**Figure**
9 **3B**). This combination was further confirmed by Chromatin isolation by RNA
10 immunoprecipitation (**Figure 3C**) experiment. In order to clarify the binding site of this
11 RNA-protein interaction, deletion-mapping experiments were performed and the results showed
12 that the 5' region of NPPA-AS1 mediated the interaction with GATA4 (**Figure 3D**). Further, this
13 combination was narrowed at 100 to 200 nt of NPPA-AS1 by RNA electrophoretic mobility shift
14 assay (EMSA), the free electrophoretic mobility of NPPA-AS1-labeled probe (100-200 nt of
15 NPPA-AS1) was blocked by recombinant GATA4, and this effect can be competitively inhibited
16 by unlabeled NPPA-AS1 probes, which demonstrated the direct interaction between NPPA-AS1
17 and GATA4 (**Figure 3E**), which demonstrated the direct interaction between NPPA-AS1 and
18 GATA4.

19 GATA4, a well-known transcription factor and a zinc finger protein, is essential for cardiac
20 development, and necessary to drive myocardial hypertrophy³⁴⁻³⁹. Indeed, inhibition of GATA4
21 expression blocked the increased cell size and transcription activation of cardiac hypertrophy
22 related genes, induced by NPPA-AS1 over-expression *in vitro* (**Figures 3F** and **3G**). The role of
23 GATA4 on the NPPA-AS1-mediated cardiac hypertrophy was further confirmed by using GATA4
24 Chromatin Immunoprecipitation-sequencing (ChIP-Seq) (**Figures 4A** and **4B**). As expected, the
25 ChIP-Seq data reminded that silencing NPPA-AS1 expression significantly repress the regulation
26 of GATA4 on gene involved in cardiac remodeling induced by PE (**Figure 4A-B** and
27 **Supplemental Figures 7A-7C**). Track view of ChIP-seq data further showed that the increased
28 deposition of GATA4 on cardiac hypertrophy and remodeling related gene's promoters induced by
29 PE, were blocked by NPPA-AS1 knock down (**Figure 4C** and **Supplemental Figure 7D**). We also
30 tested the effect of silencing NPPA-AS1 on transcription activation of cardiac hypertrophy genes,
31 induced by GATA4. We found that in the presence of NPPA-AS1 siRNA, the up-regulation of
32 those hypertrophy-related target promoter activities, mediated by GATA4, were reduced,
33 evidenced by qPCR and dual-luciferase reporter assay (**Supplemental Figures 7E** and **7F**).

34 35 **NPPA-AS1 regulates GATA4 acetylation through EP300/GATA4 interaction**

36 During cardiac hypertrophy and remodeling, GATA4 activity is significantly increased,
37 which is dictated by its acetylation status mediated by transcriptional coactivator EP300⁴⁰⁻⁴¹.
38 EP300 transfers acetyl to GATA4 amino acid residue to promote GATA4 acetylation by binding
39 with GATA4, but how EP300 binds to GATA4 is largely unknown. The above data suggest that
40 NPPA-AS1 may serve as a scaffold to bring GATA4 and EP300 together to accelerate cardiac
41 hypertrophy-related gene transcription to facilitate cardiac remodeling. Indeed, silencing of
42 NPPA-AS1 reduced GATA4 acetylation *in vitro* (**Figure 5A**), and a possible binding of EP300 and
43 NPPA-AS1 was identified through the online predictor CatRAPID (**Figure 5B**). Deletion-mapping
44 assay further demonstrated that NPPA-AS1 might interact with EP300 at 3' region (**Figure 5C**).

1 RNA EMSA assay narrowed the interaction region at 1550 to 1650 nt region of NPPA-AS1
2 **(Figure 5D)**. Similar to GATA4, recombinant EP300 could slow down mobility shift of
3 NPPA-AS1 through binding with biotin-labeled 1550-1650nt NPPA-AS1. Also, this interaction
4 was effectively competed by unlabeled 1550-1650nt NPPA-AS1 **(Figure 5D)**. Moreover, the
5 decreased GATA4 acetylation may be related to decreased interaction of GATA4 with EP300
6 because co-immunoprecipitation (co-IP) assays showed that the down regulation of NPPA-AS1
7 significantly reduced the binding of EP300 with GATA4 **(Figure 5A)**. *In vivo*, TAC could
8 significantly induce interaction between GATA4 and EP300 in WT mice and AAV9 NC shRNA
9 injected mice but failed in NPPA-AS1-inactivated mice and AAV9 NPPA-AS1 shRNA injected
10 mice **(Figures 5E and 5F)**. During cardiac hypertrophy and remodeling, NPPA-AS1 was enriched
11 on GATA4 **(Supplemental Figure 8A)**, accompanied by the increase in GATA4 acetylation
12 **(Supplemental Figure 8B)**, which was blocked by inactivating function sequence of NPPA-AS1
13 or knocking down NPPA-AS1 **(Figures 5E and 5F)**.

14 15 **Pharmacological inhibition of NPPA-AS1 *in vivo* prevents cardiac hypertrophy**

16 The above *in vivo* and *in vitro* data strongly suggest that NPPA-AS1 plays a key role in
17 cardiac remodeling. To explore its clinical translational potential, we silenced NPPA-AS1 with the
18 intraperitoneal injection of LNA-GapmeR (locked nucleic acid-GapmeR) one day after TAC and
19 weekly, thereafter, for up to 5 weeks **(Figures 6A and 6B)**. Our study showed that
20 down-regulation of NPPA-AS1 by GapmeR prevented the TAC-induced cardiac hypertrophy,
21 proved by the heart weight and body weight ratio **(Figure 6C)**, heart size **(Figure 6D)**, ventricular
22 and interventricular septal thickness **(Figure 6D)**, cardiomyocyte size **(Figures 6D and 6E)**, and
23 cardiac fibrosis **(Figures 6D and 6F)**. In addition, reduced cardiac function and altered gene
24 expression, caused by TAC, were rescued by GapmeR-NPPA-AS1 **(Figure 6G, and**
25 **Supplemental Figure 9)**, determined by echocardiography and fetal gene expression assay.

26 Collectively, our results show that NPPA-AS1 mediated the EP300/GATA4 interaction in the
27 basal state. More NPPA-AS1s are produced in response to hypertrophy-induced stress to promote
28 acetylation of GATA4 by increasing EP300/GATA4 interaction as a scaffold. Eventually, the
29 acetylated GATA4, with increased DNA binding ability and transcriptional activity, induces the
30 transcription of hypertrophy genes to accelerate cardiac hypertrophy and remodeling **(Figure 7)**.

31
32

1 Discussion

2 LncRNAs are widely involved in gene network regulation and play key roles in many
3 biological processes and diseases⁷⁻⁹. However, the function of lncRNA in the cardiovascular
4 system, especially in cardiac remodeling, is less understood. Based on current knowledge, cardiac
5 remodeling-related lncRNAs function at different stages, at least in mice. In mice, Mhr
6 expression is downregulated to the same level from 2 days to 6 weeks after TAC²⁴, while Chaer
7 expression is progressively down regulated after TAC at the same time frame²⁵. By contrast,
8 Chast is upregulated at 4 weeks, peaks at 6 weeks, and remains elevated, although at much lower
9 levels, for 13 weeks after TAC²⁶. In our studies, cardiac NPPA-AS1 expression is up-regulated at 6
10 hours, peaks after 24 hours and remains at the peak levels for 2 weeks, and then declines to the
11 12-hour levels at the 4th and 6th week of TAC, suggesting that NPPA-AS1 is an early and lasting
12 regulator in the cardiac remodeling process. We demonstrated that the cardiac hypertrophy, *in vivo*
13 or *in vitro*, was attenuated by inactivating or knocking down NPPA-AS1. The genetic editing of
14 NPPA-AS1 suppresses the hypertrophic phenotype, suggesting that inhibition of NPPA-AS1 could
15 serve as an effective therapeutic approach to prevent or minimize cardiac hypertrophy and heart
16 failure.

17 Previous studies have shown that GATA4 is highly expressed in cardiomyocytes at different
18 stages of development and plays a key role in the heart's responses to stress by regulating the
19 transcription of several cardiac-related genes, including NPPB, and MYH7³⁴⁻³⁹. The
20 EP300-mediated acetylation of GATA4 lysine residues increases its DNA binding and
21 transcriptional activity in response to hypertrophic stimuli in cardiomyocytes⁴⁰⁻⁴¹. Previous studies
22 showed that inhibiting GATA4 expression by microRNAs or drugs limits cardiac hypertrophy⁴³⁻⁴⁵.
23 We found that NPPA-AS1 directly binds to GATA4, functioning as a scaffold. Using predictive
24 models and actual experiments, we were able to localize the GATA4-binding region to the 5'
25 region (nt 100–200) of NPPA-AS1. This would suggest that NPPA-AS1 directly binds with
26 GATA4 and subsequently recruits EP300. Indeed, RIP, ChIRP, and EMSA demonstrated that
27 NPPA-AS1 could directly bring GATA4 and EP300 together. In cardiac hypertrophy and
28 remodeling, GATA4 and EP300 act like signal-switch components, binding with NPPA-AS1, and
29 making NPPA-AS1 function as a bridge to connect GATA4 and EP300 for the transfer of cardiac
30 stress signals.

31 To understand, further, how NPPA-AS1 functions, we performed an mRNA microarray to
32 analyze target genes regulated by NPPA-AS1. GO and pathway analyses showed that knocking
33 down NPPA-AS1 in PE-treated cardiomyocytes leads to a global transcriptional reprogramming of
34 the networks. LncRNAs can regulate target genes *in trans* (on distantly located genes) or *in cis* (on
35 neighboring genes)⁴⁶. Our data revealed that NPPA-AS1 functions mainly *in trans*. In addition, we
36 also found that NPPA-AS1 interacts with other functional proteins, predicted by catRAPID
37 website. Previous studies have shown that GATA4 interacts with many cardiac
38 hypertrophy-related proteins, including HIF1A, TP53, HDAC, and FOXO1^{21,28}. Whether
39 NPPA-AS1/GATA4 complex contains other molecules⁴⁷ and if NPPA-AS1 could regulate these
40 proteins is still unclear, which need further studies. Although NPPA-AS1 is enriched on GATA4
41 protein, its expression stays at a low level under basal condition. Only during cardiac hypertrophy,
42 NPPA-AS1 expression is significantly increased to recruit more GATA4 to promote GATA4
43 acetylation, which suggests the interaction between NPPA-AS1 with GATA4 in disease is the

1 predominant mechanism for GATA4-induced pro-hypertrophic signaling.

2 To explore the function and clinical translational potential of NPPA-AS1, we inhibited
3 NPPA-AS1 expression *in vivo* using three methods. We did not observe any pathological
4 phenotype in the basal state. However, our data confirmed that the postnatal inhibition NPPA-AS1
5 expression attenuates pathological cardiac hypertrophy and remodeling. The high expression of
6 NPPA-AS1 in the heart and its weak expression in other organs or tissues facilitate its
7 cardiac-selective targeting. This characteristic is desirable in the development of human
8 NPPA-AS1 inhibitors that could be tested in human hESC-derived and induced pluripotent stem
9 cell-derived cardiomyocytes (iPS-CMs). However, additional studies to determine the
10 consequences of the inhibition of NPPA-AS1 at different time points after TAC are needed and
11 whether an NPPA-AS1 inhibitor, partially or completely, could impede the development of cardiac
12 hypertrophy should be studied further. Consistent with our results, previous studies had shown that
13 NPPA-AS1 expression was significantly increased in ventricular tissue from heart failure
14 patients⁴⁸. Our studies in NRVMs (Neonatal Rat Ventricular Myocytes) and three animal models
15 confirm that NPPA-AS1 plays an important role in cardiac remodeling *in vitro* and *in vivo* and
16 show the clinical translational potential of this lncRNA.

17 In summary, our work has identified heart-enriched NPPA-AS1 that functions in the cardiac
18 remodeling process by initiating a EP300-GATA4 axis. Which is required for the transcription of
19 hypertrophy-related genes, cardiac hypertrophy, and pathological remodeling. Interrupting the
20 EP300-GATA4 axis by inhibiting NPPA-AS1 expression is a potential therapeutic strategy in the
21 treatment of maladaptive cardiac hypertrophy and remodeling.

1 **Acknowledgments**

2 These studies were supported in part by grants from the National Natural Science
3 Foundation of China (82022005, 82102834, 31771297), National Key R&D Program of China
4 (2018YFC1312700), National Institutes of Health (5R01DK039308-31, 7R37HL023081-37,
5 5P01HL074940-11) and Key Project of Chongqing Fundamental Science and Frontier Technology
6 Research (cstc2015jcyjBX0129). We also thank Dr Yibin Wang and Dr Bing Zhang for their
7 advice and support.
8

9 **Conflicts of interest**

10 The authors declare that they have no competing interests. This manuscript is an original
11 contribution not previously published, and not under consideration for publication elsewhere.
12
13
14
15
16
17
18
19
20
21
22
23
24
25
26
27
28
29
30
31
32
33
34
35
36
37
38
39
40
41
42

1 References

- 2 1. deAlmeida AC, van Oort RJ, Wehrens XH. Transverse aortic constriction in mice. *J Vis Exp.*
3 2010
- 4 2. Berk BC, Fujiwara K, Lehoux S. Ecm remodeling in hypertensive heart disease. *J Clin Invest.*
5 2007;117:568-575
- 6 3. Hill JA, Olson EN. Cardiac plasticity. *N Engl J Med.* 2008;358:1370-1380
- 7 4. Nakamura M, Sadoshima J. Mechanisms of physiological and pathological cardiac
8 hypertrophy. *Nat Rev Cardiol.* 2018;15:387-407
- 9 5. Lompre AM, Schwartz K, d'Albis A, Lacombe G, Van Thiem N, Swynghedauw B. Myosin
10 isoenzyme redistribution in chronic heart overload. *Nature.* 1979;282:105-107
- 11 6. Izumo S, Nadal-Ginard B, Mahdavi V. Protooncogene induction and reprogramming of
12 cardiac gene expression produced by pressure overload. *Proc Natl Acad Sci U S A.*
13 1988;85:339-343
- 14 7. Tham YK, Bernardo BC, Ooi JY, Weeks KL, McMullen JR. Pathophysiology of cardiac
15 hypertrophy and heart failure: Signaling pathways and novel therapeutic targets. *Arch Toxicol.*
16 2015;89:1401-1438
- 17 8. Mercer TR, Dinger ME, Mattick JS. Long non-coding rnas: Insights into functions. *Nat Rev*
18 *Genet.* 2009;10:155-159
- 19 9. Qureshi IA, Mehler MF. Emerging roles of non-coding rnas in brain evolution, development,
20 plasticity and disease. *Nat Rev Neurosci.* 2012;13:528-541
- 21 10. Wang KC, Chang HY. Molecular mechanisms of long noncoding rnas. *Mol Cell.*
22 2011;43:904-914
- 23 11. Devaux Y, Zangrando J, Schroen B, Creemers EE, Pedrazzini T, Chang CP, Dorn GW, 2nd,
24 Thum T, Heymans S. Long noncoding rnas in cardiac development and ageing. *Nat Rev*
25 *Cardiol.* 2015;12:415-425
- 26 12. Mohammad F, Mondal T, Guseva N, Pandey GK, Kanduri C. Kcnq1ot1 noncoding rna
27 mediates transcriptional gene silencing by interacting with dnmt1. *Development.*
28 2010;137:2493-2499
- 29 13. Michalik KM, You X, Manavski Y, Doddaballapur A, Zornig M, Braun T, John D,
30 Ponomareva Y, Chen W, Uchida S, Boon RA, Dimmeler S. Long noncoding rna malat1
31 regulates endothelial cell function and vessel growth. *Circ Res.* 2014;114:1389-1397
- 32 14. Grote P, Wittler L, Hendrix D, Koch F, Wahrisch S, Beisaw A, Macura K, Blass G, Kellis M,
33 Werber M, Herrmann BG. The tissue-specific lncrna fendrr is an essential regulator of heart
34 and body wall development in the mouse. *Dev Cell.* 2013;24:206-214
- 35 15. Puvvula PK, Desetty RD, Pineau P, Marchio A, Moon A, Dejean A, Bischof O. Long
36 noncoding rna panda and scaffold-attachment-factor safa control senescence entry and exit.
37 *Nat Commun.* 2014;5:5323
- 38 16. Li W, Notani D, Ma Q, Tanasa B, Nunez E, Chen AY, Merkurjev D, Zhang J, Ohgi K, Song X,
39 Oh S, Kim HS, Glass CK, Rosenfeld MG. Functional roles of enhancer rnas for
40 oestrogen-dependent transcriptional activation. *Nature.* 2013;498:516-520
- 41 17. Ponting CP, Oliver PL, Reik W. Evolution and functions of long noncoding rnas. *Cell.*
42 2009;136:629-641
- 43 18. Batista PJ, Chang HY. Long noncoding rnas: Cellular address codes in development and
44 disease. *Cell.* 2013;152:1298-1307

-
- 1 19. Adams BD, Parsons C, Walker L, Zhang WC, Slack FJ. Targeting noncoding rnas in disease. *J*
2 *Clin Invest.* 2017;127:761-771
- 3 20. Helgadóttir A, Thorleifsson G, Manolescu A, Gretarsdóttir S, Blondal T, Jonasdóttir A,
4 Jonasdóttir A, Sigurdsson A, Baker A, Pálsson A, Masson G, Gudbjartsson DF, Magnusson KP,
5 Andersen K, Levey AI, Backman VM, Matthíasdóttir S, Jónsdóttir T, Pálsson S, Einarsson H,
6 Gunnarsdóttir S, Gylfason A, Vaccarino V, Hooper WC, Reilly MP, Granger CB, Austin H,
7 Rader DJ, Shah SH, Quyyumi AA, Gulcher JR, Thorgeirsson G, Thorsteinsdóttir U, Kong A,
8 Stefansson K. A common variant on chromosome 9p21 affects the risk of myocardial
9 infarction. *Science.* 2007 ;316(5830):1491-3.
- 10 21. Wu G, Cai J, Han Y, Chen J, Huang ZP, Chen C, Cai Y, Huang H, Yang Y, Liu Y, Xu Z, He D,
11 Zhang X, Hu X, Pinello L, Zhong D, He F, Yuan GC, Wang DZ, Zeng C. Lincrna-p21
12 regulates neointima formation, vascular smooth muscle cell proliferation, apoptosis, and
13 atherosclerosis by enhancing p53 activity. *Circulation.* 2014;130:1452-1465
- 14 22. Klattenhoff CA, Scheuermann JC, Surface LE, Bradley RK, Fields PA, Steinhauser ML, Ding
15 H, Butty VL, Torrey L, Haas S, Abo R, Tabebordbar M, Lee RT, Burge CB, Boyer LA.
16 Braveheart, a long noncoding rna required for cardiovascular lineage commitment. *Cell.*
17 2013;152:570-583
- 18 23. Grote P, Wittler L, Hendrix D, Koch F, Wahrlich S, Beisaw A, Macura K, Blass G, Kellis M,
19 Werber M, Herrmann BG. The tissue-specific lncrna fendrr is an essential regulator of heart
20 and body wall development in the mouse. *Dev Cell.* 2013; 24(2):206-214
- 21 24. Han P, Li W, Lin CH, Yang J, Shang C, Nuernberg ST, Jin KK, Xu W, Lin CY, Lin CJ, Xiong
22 Y, Chien H, Zhou B, Ashley E, Bernstein D, Chen PS, Chen HV, Quertermous T, Chang CP. A
23 long noncoding rna protects the heart from pathological hypertrophy. *Nature.*
24 2014;514:102-106
- 25 25. Wang Z, Zhang XJ, Ji YX, Zhang P, Deng KQ, Gong J, Ren S, Wang X, Chen I, Wang H, Gao
26 C, Yokota T, Ang YS, Li S, Cass A, Vondriská TM, Li G, Deb A, Srivastava D, Yang HT, Xiao
27 X, Li H, Wang Y. The long noncoding rna chaer defines an epigenetic checkpoint in cardiac
28 hypertrophy. *Nat Med.* 2016;22:1131-1139
- 29 26. Viereck J, Kumarswamy R, Foinquinos A, Xiao K, Avramopoulos P, Kunz M, Dittrich M,
30 Maetzig T, Zimmer K, Remke J, Just A, Fendrich J, Scherf K, Bolesani E, Schambach A,
31 Weidemann F, Zweigerdt R, de Windt LJ, Engelhardt S, Dandekar T, Batkai S, Thum T. Long
32 noncoding rna chast promotes cardiac remodeling. *Sci Transl Med.* 2016;8:326ra322
- 33 27. Hashimoto H, Olson EN, Bassel-Duby R. Therapeutic approaches for cardiac regeneration and
34 repair. *Nat Rev Cardiol.* 2018 :585-600
- 35 28. Kong L, Zhang Y, Ye ZQ, Liu XQ, Zhao SQ, Wei L, Gao G. CPC: Assess the protein-coding
36 potential of transcripts using sequence features and support vector machine. *Nucleic Acids*
37 *Res.* 2007;35:W345-349
- 38 29. Wang L, Park HJ, Dasari S, Wang S, Kocher JP, Li W. Cpat: Coding-potential assessment tool
39 using an alignment-free logistic regression model. *Nucleic Acids Res.* 2013;41:e74
- 40 30. Huang ZP, Kataoka M, Chen J, Wu G, Ding J, Nie M, Lin Z, Liu J, Hu X, Ma L, Zhou B,
41 Wakimoto H, Zeng C, Kyselovic J, Deng ZL, Seidman CE, Seidman JG, Pu WT, Wang DZ.
42 Cardiomyocyte-enriched protein CIP protects against pathophysiological stresses and
43 regulates cardiac homeostasis. *J Clin Invest.* 2015;125:4122-4134
- 44 31. Quinodoz S, Guttman M. Long noncoding rnas: An emerging link between gene regulation

-
- 1 and nuclear organization. *Trends Cell Biol.* 2014;24:651-663
- 2 32. Meller VH, Joshi SS, Deshpande N. Modulation of chromatin by noncoding RNA. *Annu Rev*
3 *Genet.* 2015;49:673-695
- 4 33. Bellucci M, Agostini F, Masin M, Tartaglia GG. Predicting protein associations with long
5 noncoding rnas. *Nat Methods.* 2011;8:444-445
- 6 34. Molkenin JD, Olson EN. Gata4: A novel transcriptional regulator of cardiac hypertrophy?
7 *Circulation.* 1997;96:3833-3835
- 8 35. Molkenin JD. The zinc finger-containing transcription factors gata-4, -5, and -6. Ubiquitously
9 expressed regulators of tissue-specific gene expression. *J Biol Chem.* 2000;275:38949-38952
- 10 36. Hasegawa K, Lee SJ, Jobe SM, Markham BE, Kitsis RN. Cis-acting sequences that mediate
11 induction of beta-myosin heavy chain gene expression during left ventricular hypertrophy due
12 to aortic constriction. *Circulation.* 1997;96:3943-3953
- 13 37. Perrino C, Rockman HA. Gata4 and the two sides of gene expression reprogramming. *Circ*
14 *Res.* 2006;98:715-716
- 15 38. He A, Gu F, Hu Y, Ma Q, Ye LY, Akiyama JA, Visel A, Pennacchio LA, Pu WT. Dynamic
16 gata4 enhancers shape the chromatin landscape central to heart development and disease. *Nat*
17 *Commun.* 2014;5:4907
- 18 39. Oka T, Maillet M, Watt AJ, Schwartz RJ, Aronow BJ, Duncan SA, Molkenin JD.
19 Cardiac-specific deletion of gata4 reveals its requirement for hypertrophy, compensation, and
20 myocyte viability. *Circ Res.* 2006;98:837-845
- 21 40. Dai YS, Markham BE. P300 functions as a coactivator of transcription factor gata-4. *J Biol*
22 *Chem.* 2001;276:37178-37185
- 23 41. Takaya T, Kawamura T, Morimoto T, Ono K, Kita T, Shimatsu A, Hasegawa K. Identification
24 of P300-targeted acetylated residues in gata4 during hypertrophic responses in cardiac
25 myocytes. *J Biol Chem.* 2008;283:9828-9835
- 26 42. Vlieghe D, Sandelin A, De Bleser PJ, Vleminckx K, Wasserman WW, van Roy F, Lenhard B.
27 A new generation of jasper, the open-access repository for transcription factor binding site
28 profiles. *Nucleic Acids Res.* 2006;34:D95-97
- 29 43. Ikeda S, He A, Kong SW, Lu J, Bejar R, Bodyak N, Lee KH, Ma Q, Kang PM, Golub TR, Pu
30 WT. MicroRNA-1 negatively regulates expression of the hypertrophy-associated calmodulin and
31 mef2a genes. *Mol Cell Biol.* 2009;29:2193-2204
- 32 44. Han M, Yang Z, Sayed D, He M, Gao S, Lin L, Yoon S, Abdellatif M. Gata4 expression is
33 primarily regulated via a mir-26b-dependent post-transcriptional mechanism during cardiac
34 hypertrophy. *Cardiovasc Res.* 2012;93:645-654
- 35 45. Liu Y, Wang Z, Xiao W. MicroRNA-26a protects against cardiac hypertrophy via inhibiting
36 gata4 in rat model and cultured cardiomyocytes. *Mol Med Rep.* 2016;14:2860-2866
- 37 46. Rinn JL, Chang HY. Genome regulation by long noncoding rnas. *Annu Rev Biochem.*
38 2012;81:145-166
- 39 47. Dai YS, Markham BE. P300 functions as a coactivator of transcription factor gata-4. *J Biol*
40 *Chem.* 2001;276:37178-37185
- 41 48. Celik S, Sadegh MK, Morley M, Roselli C, Ellinor PT, Cappola T, Smith JG, Gidlöf O.
42 Antisense regulation of atrial natriuretic peptide expression. *JCI Insight.* 2019;4(19):e130978.
- 43
44

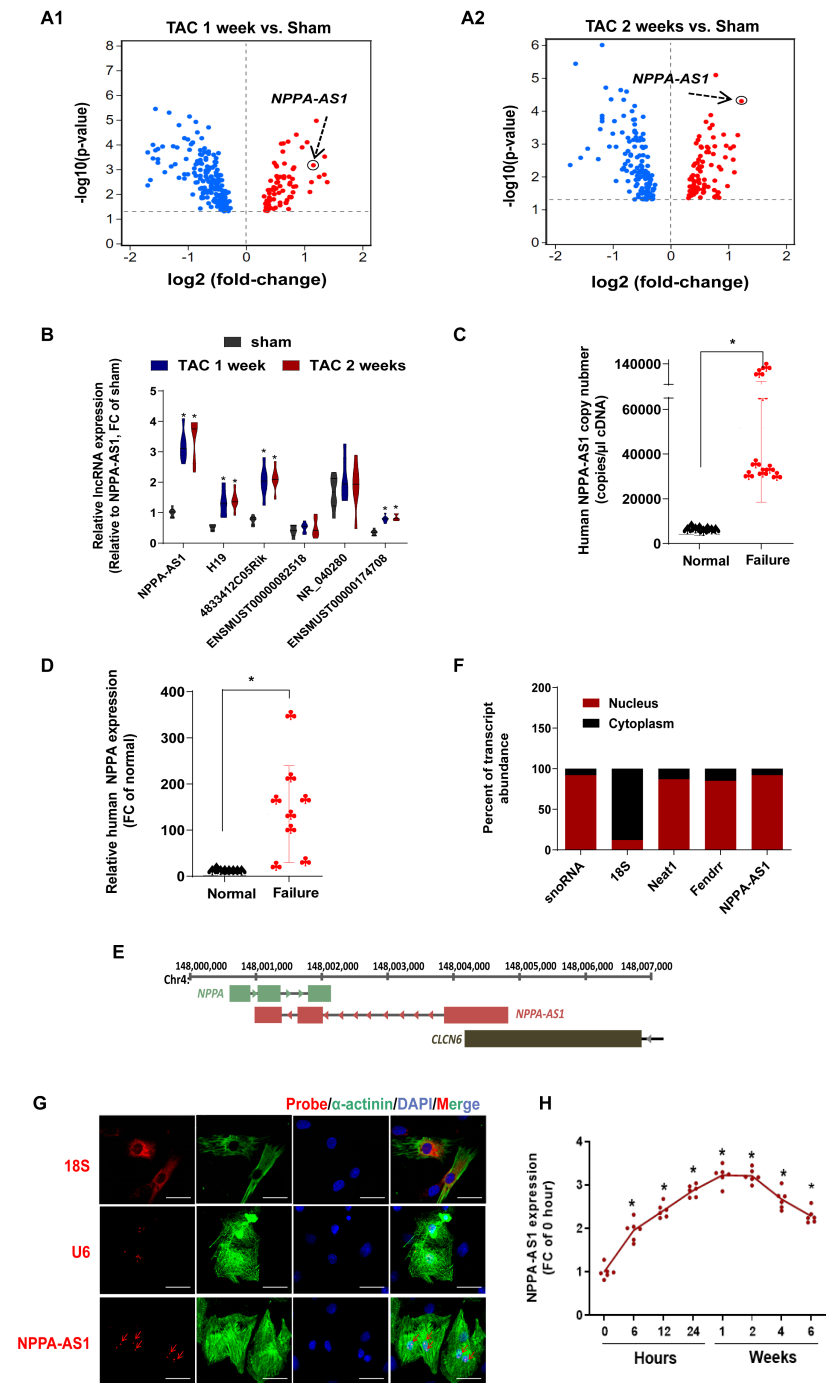


Figure 1

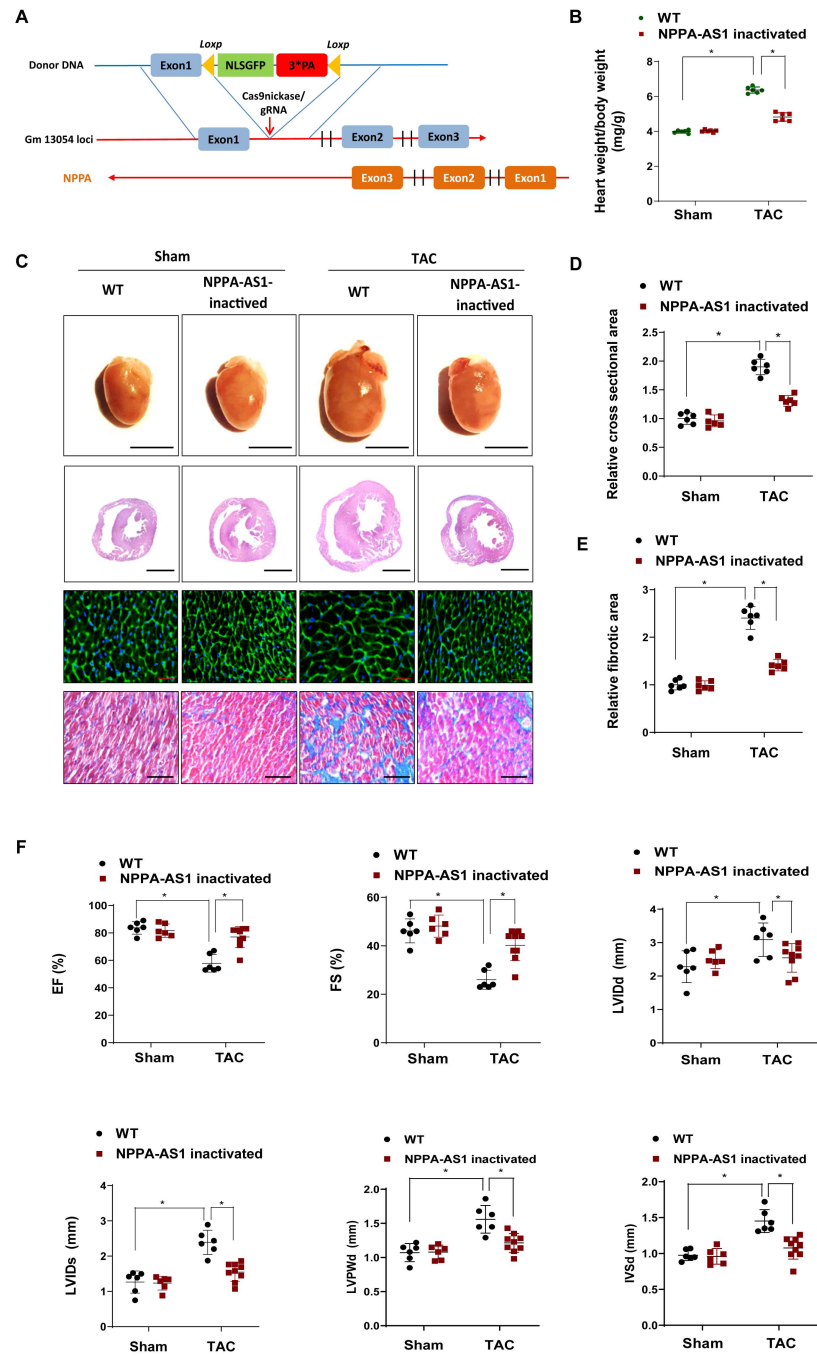


Figure 2

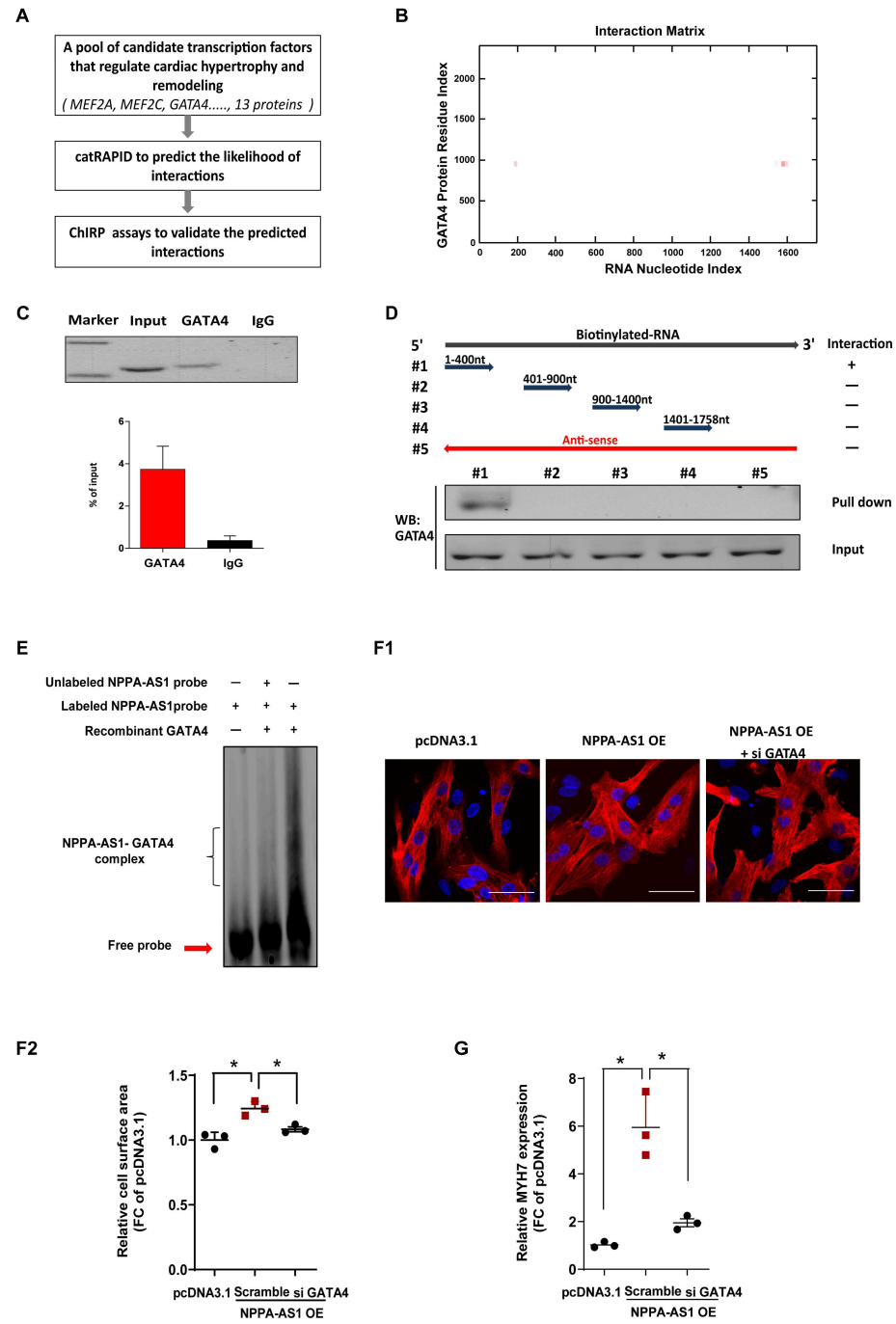
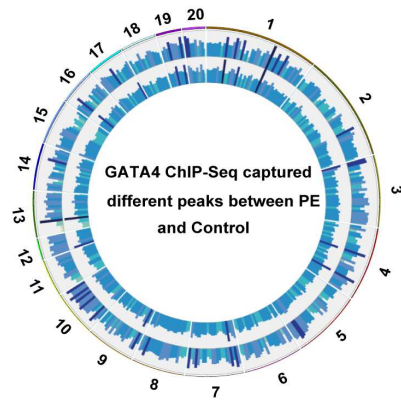
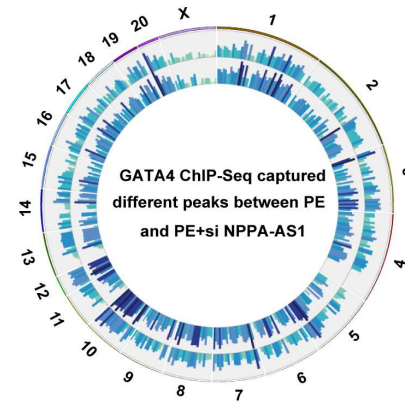


Figure 3

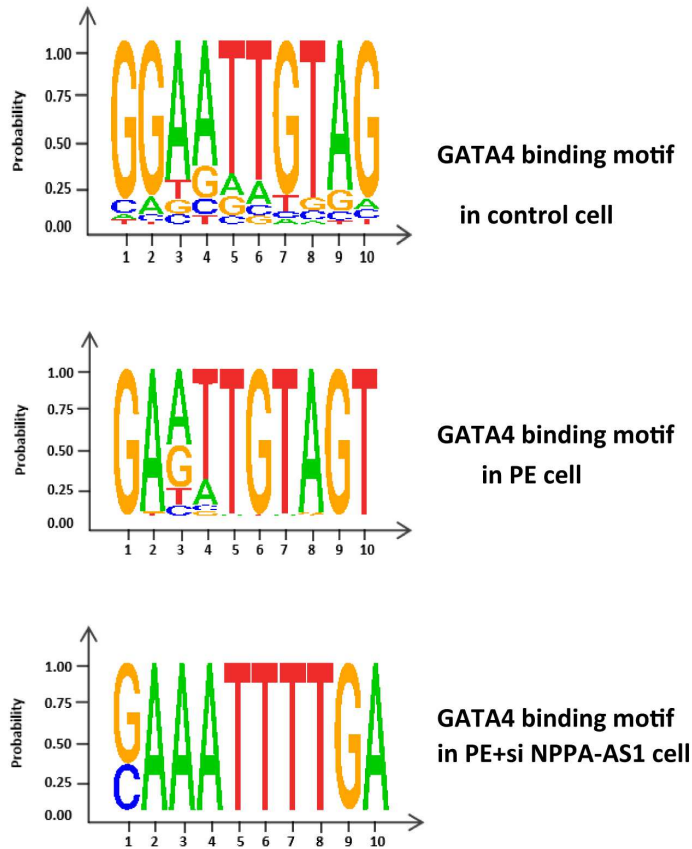
A1



A2



B



C

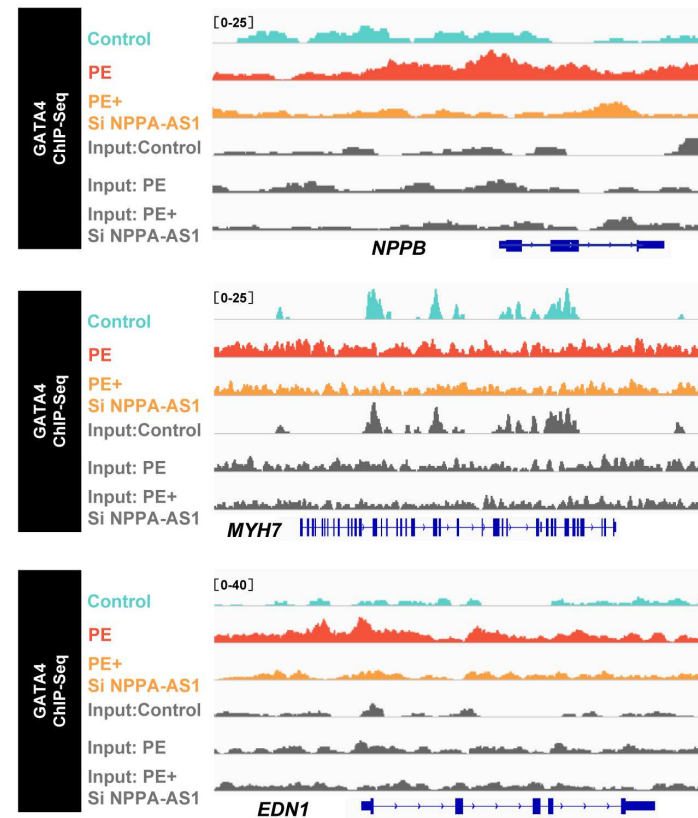
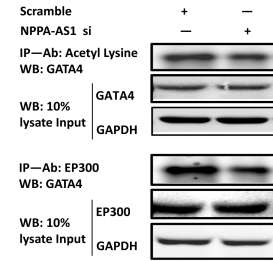
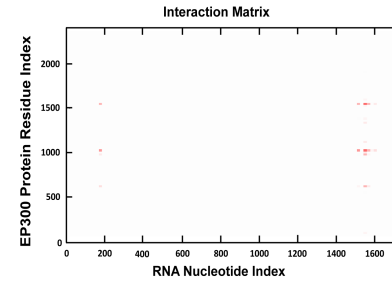


Figure 4

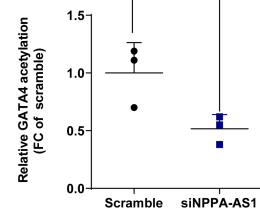
A1



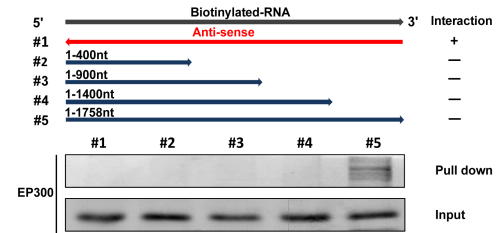
B



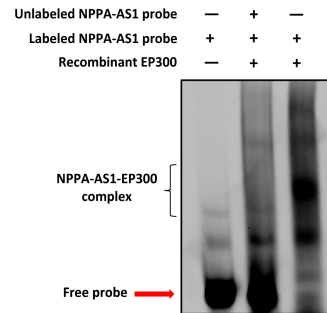
A2



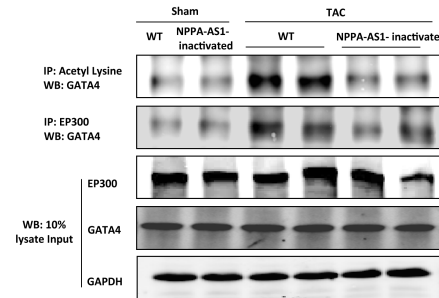
C



D



E



F

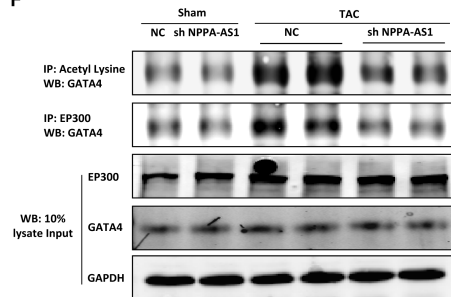


Figure 5

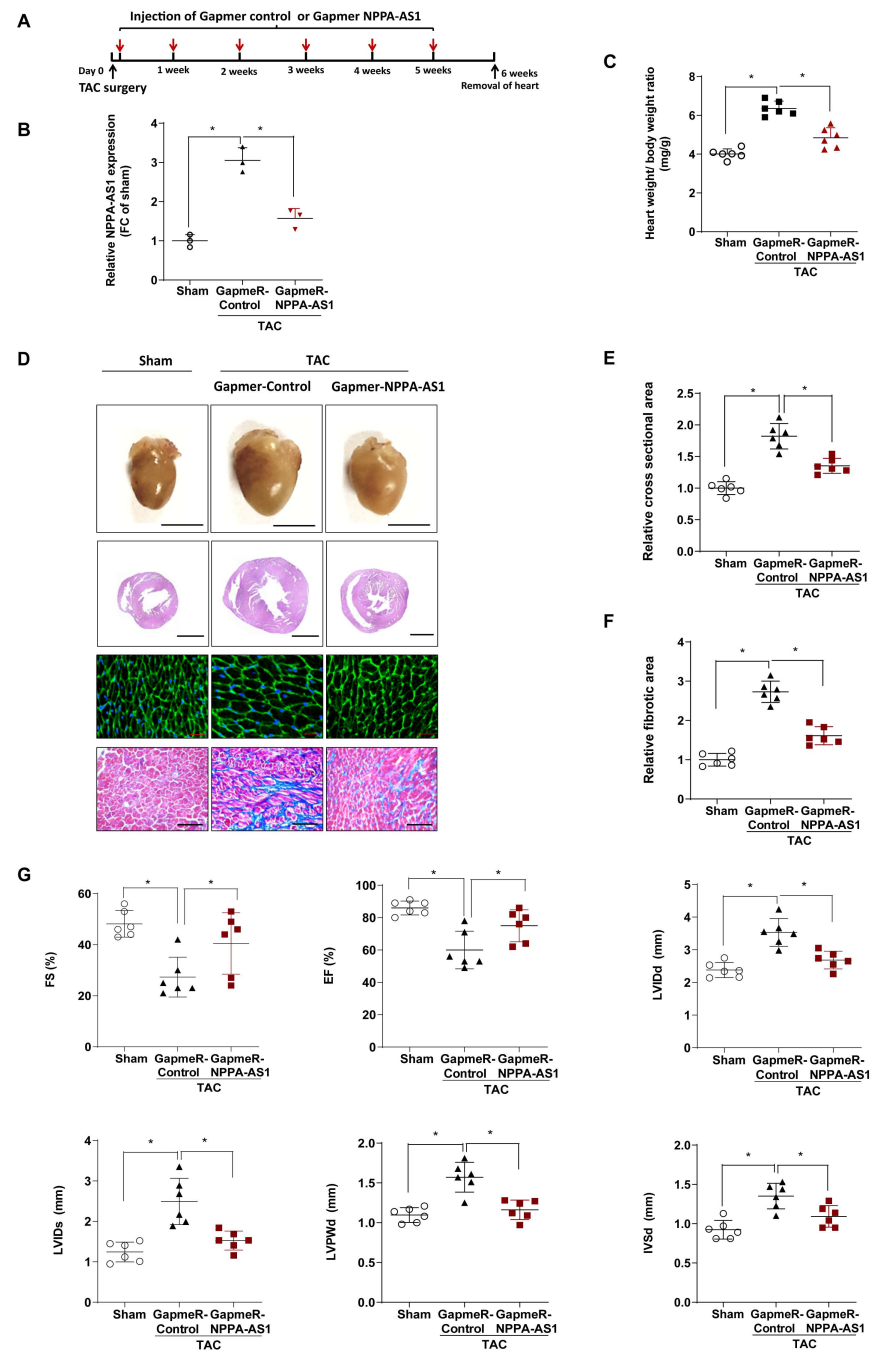


Figure 6

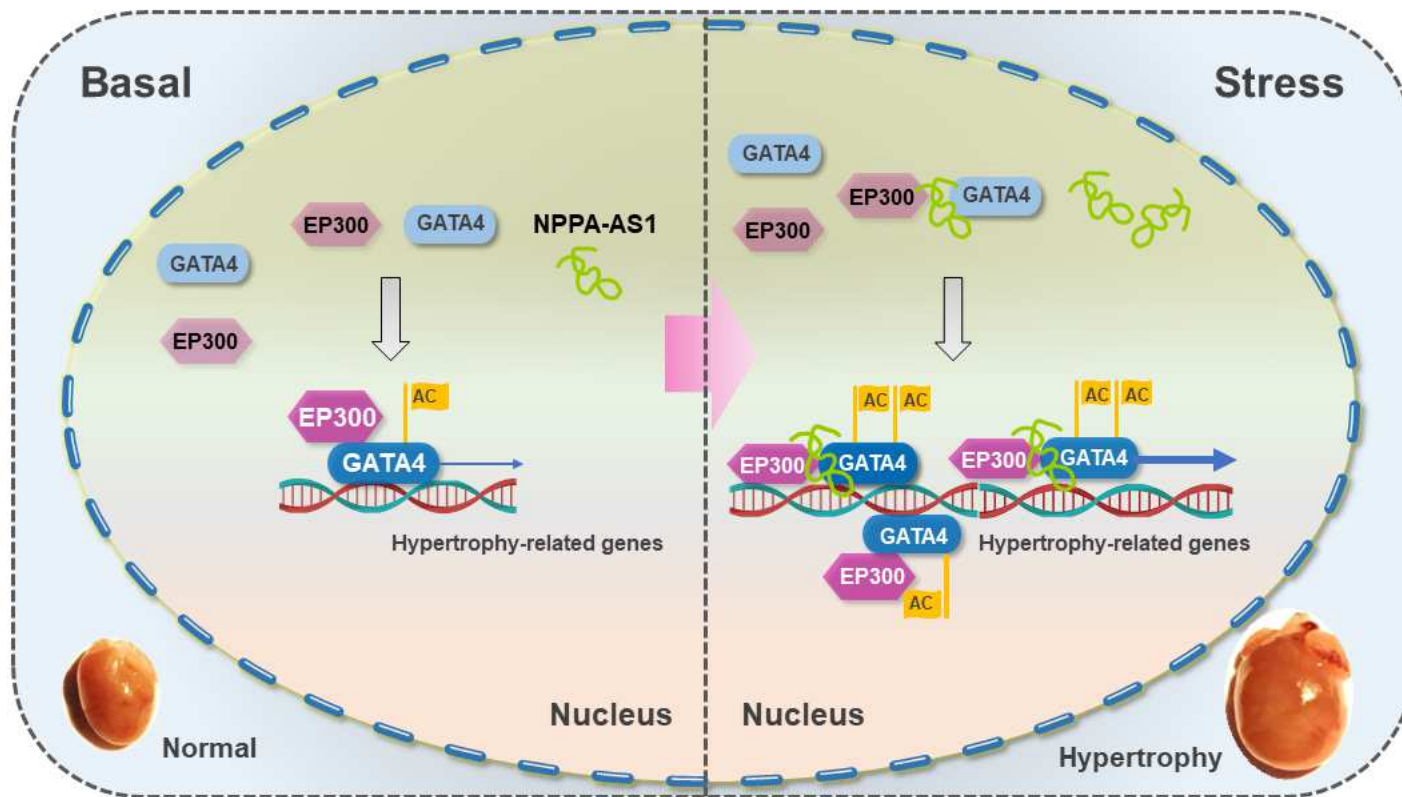


Figure 7

Figure legends:

Figure 1. NPPA-AS1 is a cardiac-enriched and hypertrophy-associated lncRNA.

(A) Volcano plot showing the clustering of lncRNAs differentially expressed in hearts after TAC 1 week and 2 weeks [fold-change (FC) > 1.2], relative to sham-operated hearts. The red and blue dots indicate up or down regulated lncRNAs in TAC hearts respectively. (B) Validation of selected lncRNAs in hearts after 1 and 2 weeks of TAC. Data are mean fold-change (FC) relative to NPPA-AS1 sham \pm SD (n = 6). *P < 0.05 versus respective sham, one-way ANOVA, Holm-Sidak test. (C) NPPA-AS1 copy number in normal hearts and in hearts with cardiac failure, RNAs isolated from heart tissues were used to perform digital PCR to calculate the NPPA-AS1 copy number in per μ l cDNA. N = 8 each for cardiac failure and normal heart group. (D) NPPA expressions in normal hearts and in hearts with cardiac failure, RNAs isolated from heart tissues were subjected to real-time qPCR to detect NPPA expression levels, n = 8 each for cardiac failure and normal heart group. Data are mean fold-change (FC) relative to normal \pm SD. Data are mean fold-change (FC) relative to normal \pm SD. (D and E) *P < 0.05, Student's t-test. (E) Schematic illustration of NPPA-AS1 RNA originating from the antisense of NPPA gene and CLCN6 gene. (F) Real-time qPCR of nuclear/cytoplasmic RNA in cardiomyocytes. 18S RNA is primarily cytoplasmic RNA whereas snoRNA, Neat1 and Fendrr, are nuclear lncRNAs, which are taken as controls. (G) Fluorescence in situ hybridization (FISH), Red: probe for 18s snRNA (18s), U6 snRNA (U6), and NPPA-AS1; green: α -actinin; blue: DAPI (bars, 50 μ m). (H) NPPA-AS1 expression at different time points of TAC. Data are mean fold-change (FC) relative to 0 hour \pm SD (n = 6), *P < 0.05 versus 0-hour, one-way ANOVA, Holm-Sidak test.

Figure 2. NPPA-AS1 is required for pressure overload-induced cardiac hypertrophy and remodeling.

(A) Rationale for the inactivation of NPPA-AS1 in mouse heart. To generate NPPA-AS1-function-sequence exon3-inactivated mice, CRISPR-Cas9 editing approach was used. 3* poly A sequence was inserted behind Exon 1 of NPPA-AS1 to inhibit transcription of Exon 2 and Exon 3 to create premature termination of the NPPA-AS1. GFP was inserted in front of poly A to trace the inserted sequence. LoxP was also used for removing inserted DNA sequence in further studies. 3*PA: 3X poly adenylate tail. NLSGFP = nuclear localization signal green fluorescent protein. (B) Heart weight/body weight ratio (n = 6). Data are mean \pm SD. (C) Gross morphology (bars, 5 mm), histological analysis using hematoxylin and eosin staining (bars, 2 mm), transverse sections analysis using wheat germ agglutinin staining (bars, 20 μ m) and fibrosis analysis using masson trichrome staining (bars, 500 μ m), of adult hearts from NPPA-AS1-inactivated and WT mice 6 weeks after TAC or sham. (D) Quantification of the size of cardiomyocytes by measurement of transverse cell area, Data are mean fold-change (FC) relative to WT sham \pm SD. (n = 6). (E) Quantification of the stained fibrosis area, Data are mean fold-change (FC) relative to WT sham \pm SD. (n = 6). (F) Echocardiographic analyses of cardiac function of adult hearts from NPPA-AS1-inactivated and WT mice 6 weeks after TAC or sham. Data are mean \pm SD, n = 6 for WT sham, NPPA-AS1-inactivated sham groups, WT TAC, n = 9 for NPPA-AS1-inactivated TAC group. EF = left ventricular ejection fraction; FS = fractional shortening; LVIDd = left ventricular internal dimension at diastole. LVIDs = left ventricular internal dimension at systole. LVPWd = Left ventricular posterior wall at diastole; IVSd = Interventricular septal at diastole. WT: wild-type. *P < 0.05, two way ANOVA, Holm-Sidak test.

Figure 3. GATA4 physically interacts with NPPA-AS1 and functions as the effector of NPPA-AS1.

(A) Selection strategy of candidate effectors for NPPA-AS1 in regulating cardiac hypertrophy and remodeling. Cardiac hypertrophy and remodeling related transcription factors were selected to build a candidate pool, followed by computational prediction and experimental validation using chromatin isolation by RNA purification (ChIRP) assays. (B) Predicted interaction of NPPA-AS1 RNA (nucleotide positions) and GATA4 protein (amino acid residues) using catRAPID (http://big.crg.cat/gene_function_and_evolution/services/catrapid). (C) Interaction of NPPA-AS1 and GATA4. RNA immunoprecipitation experiments were performed using GATA4 antibody in mouse cardiomyocytes lysates. Associated NPPA-AS1 was detected by regular RT-PCR. Real-time qPCR quantified the enrichment of pulled-down NPPA-AS1 by GATA4. IgG was used as negative control. Data are mean percentage of input (n = 3). (D) Biotinylated RNA streptavidin pull-down mapping the GATA4 interaction region of NPPA-AS1. Truncated NPPA-AS1 RNAs were co-incubated with mouse cardiomyocyte lysates, and the pull-down products were detected by western blotting. (E) RNA electrophoretic mobility shift assay (EMSA) analysis for detecting the interaction between NPPA-AS1 and GATA4 *in vitro*. Recombinant GATA4s were incubated with biotin-labeled NPPA-AS1 probe, with or without unlabeled probe. 100-200 nt of NPPA-AS1 was used to produce labeled or unlabeled probe. Unlabeled NPPA-AS1 probe was used for specific competitor in biotin-labeled NPPA-AS1 and GATA4 binding reaction. (F) Cell sizes of NRVMs transduced with pcDNA3.1, NPPA-AS1 over-expression plasmids, or GATA4 siRNA (bars, 50 μ m). Red: α -actinin, Blue: DAPI (n = 6). (G) Fetal gene MYH7 expression. Data are mean fold-change (FC), relative to pcDNA3.1 \pm SD. *P < 0.05, one-way ANOVA, Holm-Sidak test.

Figure 4. NPPA-AS1 regulates the GATA4-dependent transcription of target genes.

(A) Distribution of GATA4 ChIP-Seq captured different peaks between PE and control and different peaks between PE + si NPPA-AS1 and PE, peaks were aligned according to chromosome position in the circle. (B) Representative GATA4 and NPPA-AS1 binding motif in cardiomyocytes. (C) Visualization of GATA4 ChIP-Seq data tracks. Cardiac hypertrophy and remodeling related genes were selected and IGV screen shots was used to show representative peaks, included NPPB, MYH7 and EDN1.

Figure 5. NPPA-AS1 regulates GATA4 acetylation through EP300/GATA4 interaction.

(A1) Effect of NPPA-AS1 on GATA4 acetylation through EP300/GATA4 interaction *in-vitro*. Co-IP assays were performed to detect the acetylation of GATA4 and interaction of EP300/GATA4. Cardiomyocytes were transfected with NPPA-AS1 siRNA or scramble siRNA. The cell lysates were co-incubated with acetyl lysine or EP300 antibodies. Associated proteins were detected using GATA4 antibodies. 10% input lysates were used as loading control through detecting EP300 and GAPDH expression. (n = 3). (A2) Count of inhibition efficacy of siRNA on GATA4 acetylation as that in figure A1. (B) Predicted interaction of NPPA-AS1 RNA (nucleotide positions) and EP300 protein (amino acid residues) using catRAPID (http://big.crg.cat/gene_function_and_evolution/services/catrapid). (C) Biotinylated RNA streptavidin pulldown mapping the EP300 interaction region of NPPA-AS1. Full-length and

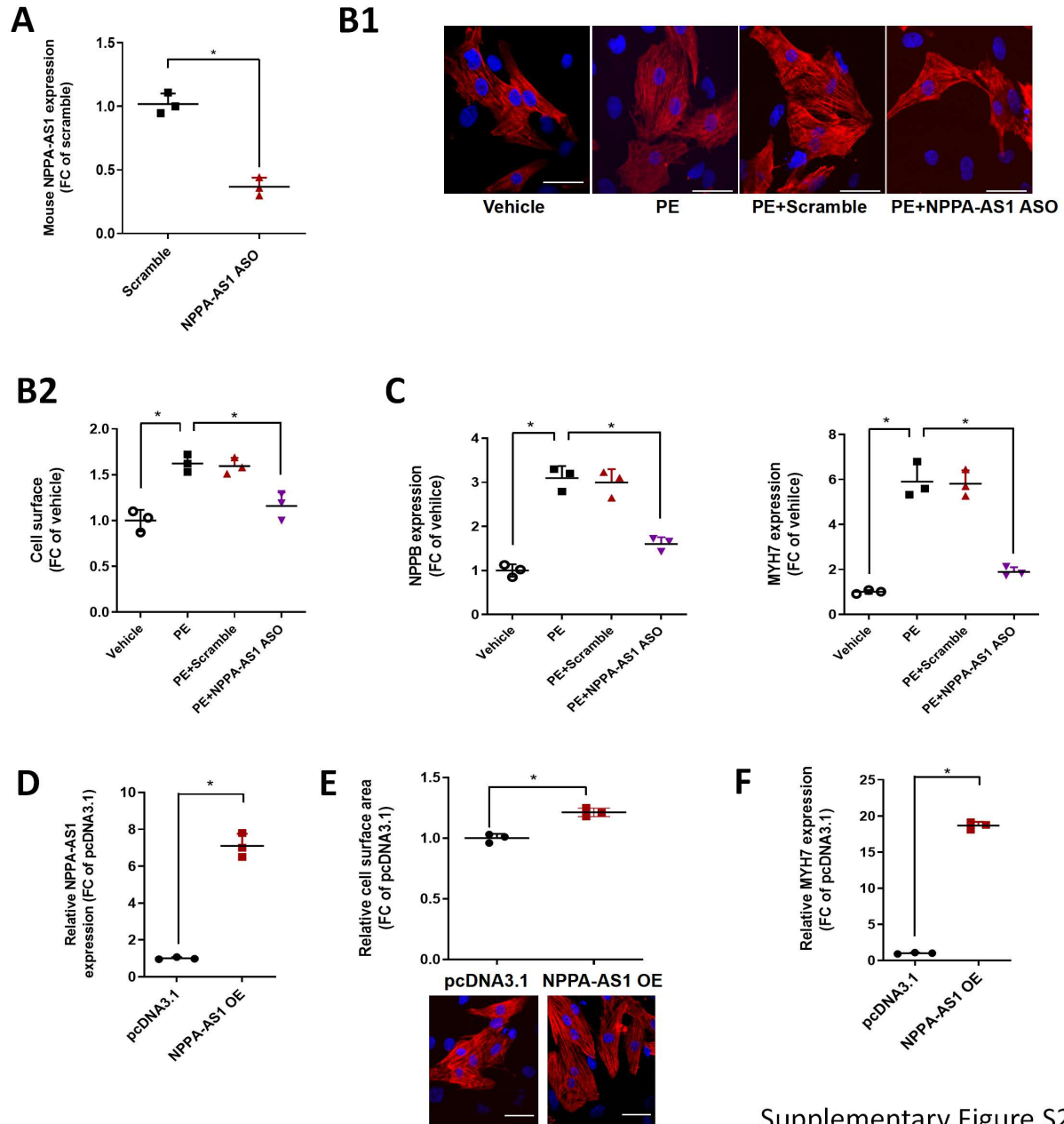
truncated NPPA-AS1 RNAs were co-incubated with mouse cardiomyocyte lysates, and the pull-down products were detected by western blotting. (D) RNA EMSA for detecting the interaction between NPPA-AS1 and EP300 *in vitro*. Recombinant EP300 were incubated with biotin-labeled NPPA-AS1 probe, with or without unlabeled probe. Unlabeled NPPA-AS1 probe was used for specific competitor in biotin-labeled NPPA-AS1 and EP300 binding reaction. (E-F) Effect of NPPA-AS1 on GATA4 acetylation through EP300/GATA4 interaction *in-vivo*. Co-IPs were performed to detect the acetylation of GATA4 and the interaction of EP300 and GATA4 in NPPA-AS1-inactivated mice and sh NPPA-AS1 mice 6 weeks after TAC or sham. Acetyl lysine and EP300 antibodies were used for immunoprecipitation (IP-Ab) and GATA4 antibody was used for immunoblotting (IB-Ab).

Figure 6. Pharmacological inhibition of NPPA-AS1 *in vivo* prevents cardiac remodeling.

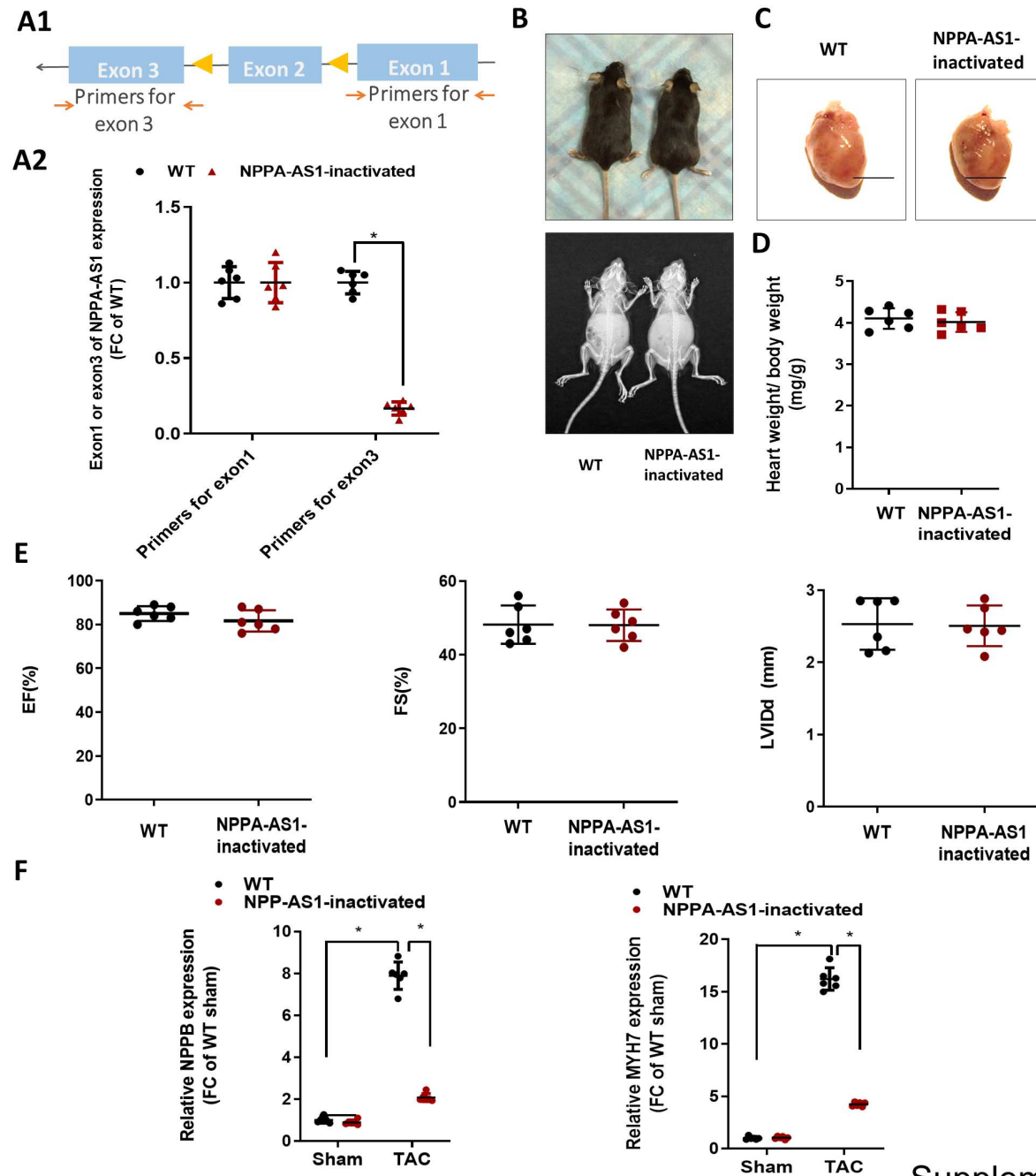
(A) Overview of the experimental setup with six weekly intraperitoneal injection of GapmeR-control (scrambled sequence) or GapmeR-NPPA-AS1, starting at day 1 after TAC until removal of the heart after 6 weeks. (B) NPPA-AS1 expression in GapmeR-control- or GapmeR-NPPA-AS1-treated mouse hearts, after sham or TAC for 6 weeks, expressions were quantified by real-time qPCR. (n = 3). (C) Heart weight/body weight ratio of mice performed with sham or TAC surgery. Mice with TAC were intraperitoneal injection of GapmeR-control- or GapmeR-NPPA-AS1 for 6 weeks (n = 6). Data are mean \pm SD. (D) Gross morphology (bars, 5 mm), histological analysis using hematoxylin and eosin staining (bars, 2 mm), transverse sections analysis using wheat germ agglutinin staining (bars, 20 μ m) and fibrosis analysis using masson trichrome staining (bars, 500 μ m), of adult hearts from GapmeR-control- and GapmeR-NPPA-AS1-treated mice after TAC or sham. (E) Quantification of the size of cardiomyocytes by measurement of transverse cell area, Data are mean fold-change (FC) relative to sham \pm SD. (n = 6). (F) Quantification of the stained fibrosis area, Data are mean fold-change (FC) relative to sham \pm SD. (n = 6). (G) Echocardiographic analyses for cardiac function of adult hearts from GapmeR-control- or GapmeR-NPPA-AS1- treated mice (n = 6). Data are mean fold-change (FC) relative to sham \pm SD. EF = left ventricular ejection fraction; FS = fractional shortening; LVIDd = left ventricular internal dimension at diastole. LVIDs = left ventricular internal dimension at systole. *P < 0.05; one-way ANOVA, Holm-Sidak test.

Figure 7. Working model of a NPPA-AS1 mediated EP300-GATA4 axis in the heart.

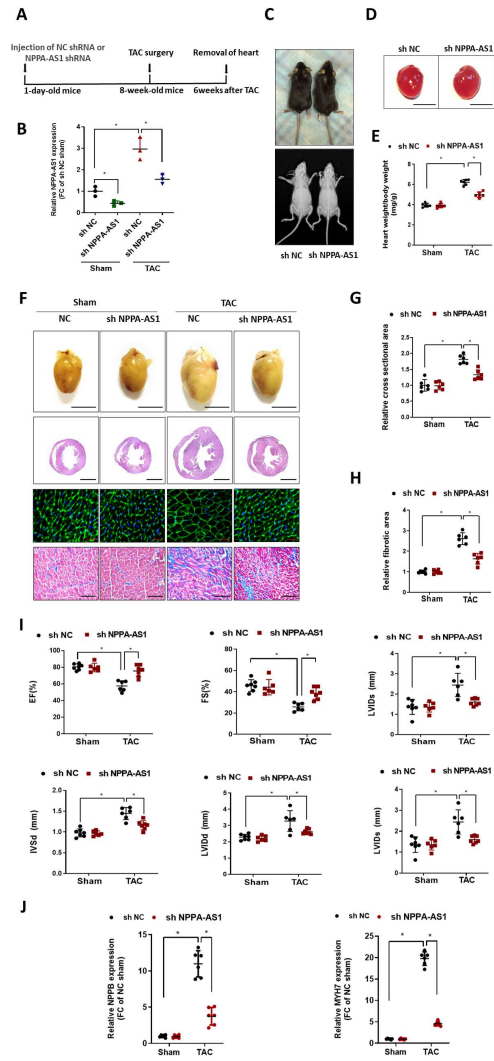
In the basal state, NPPA-AS1 can mediate EP300/GATA4 interaction. In response to hypertrophic stress, more NPPA-AS1 are produced. This promotes acetylation of GATA4 by increasing EP300/GATA4 interaction as a scaffold. Finally, the acetylated GATA4, with increased DNA binding ability and transcriptional activity, induces the transcription of hypertrophy genes that accelerate cardiac hypertrophy and remodeling.



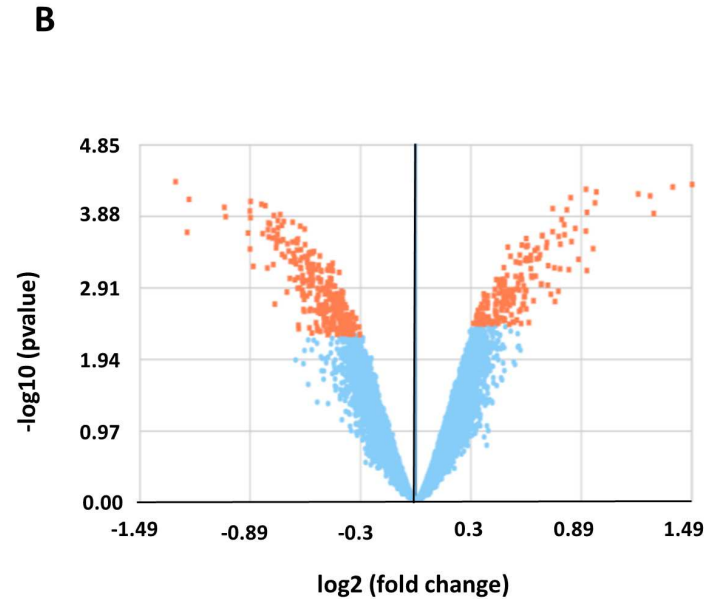
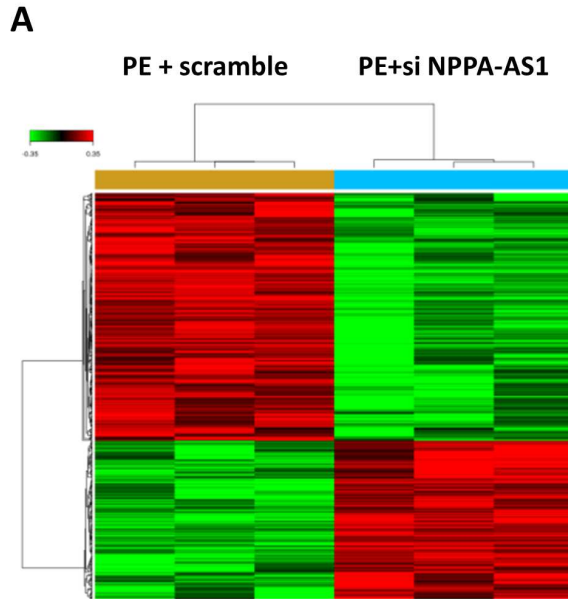
Supplementary Figure S2



Supplementary Figure S3



Supplementary Figure S4

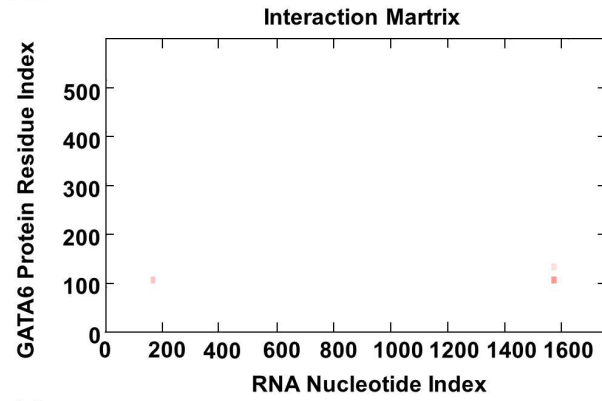
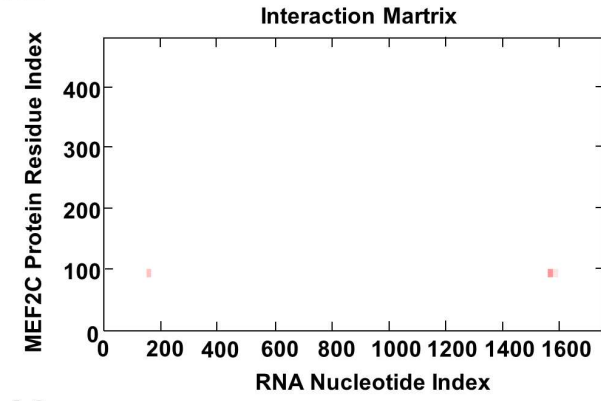
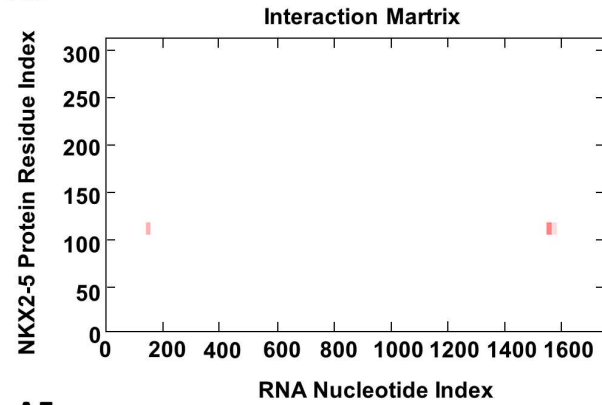
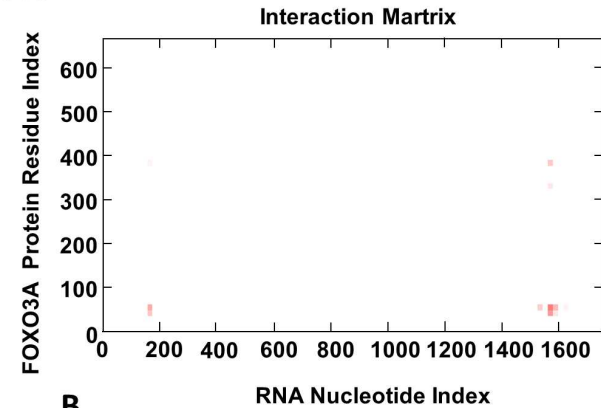
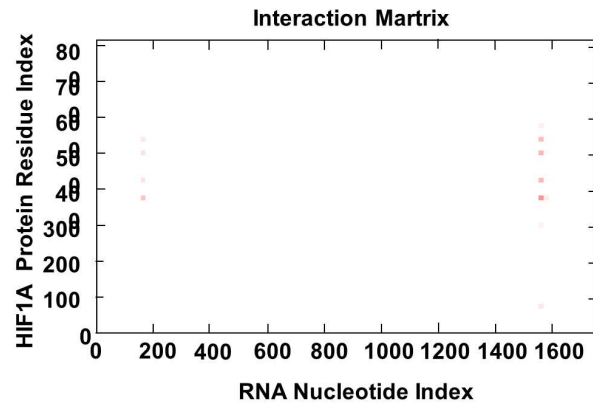
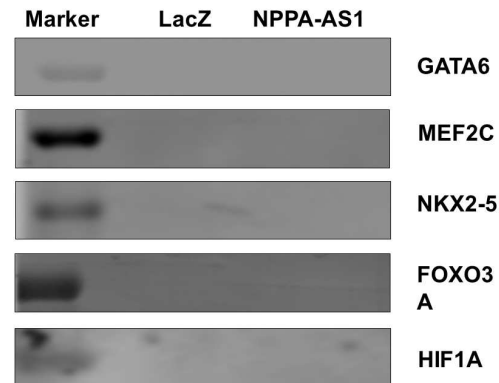


C **Pathway analysis , top changed**

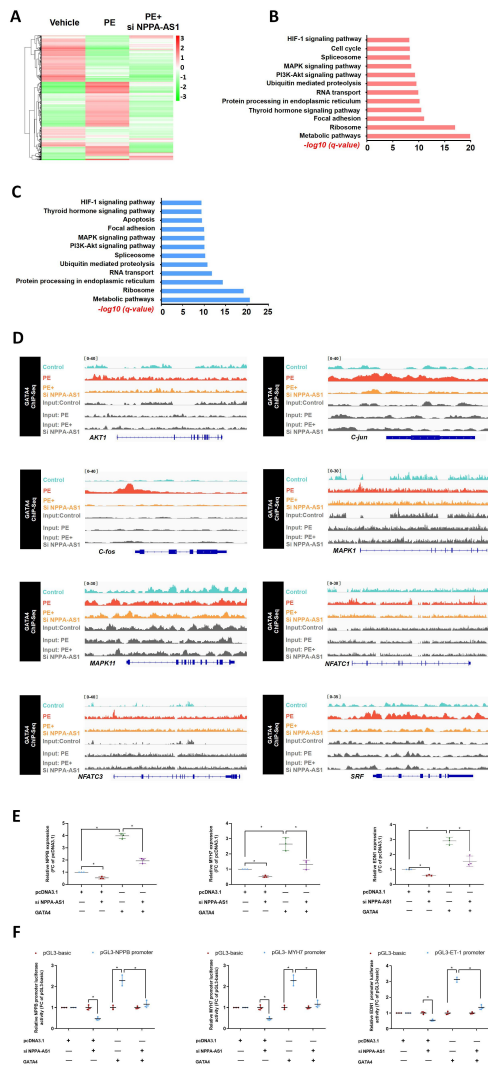
1. Influenza A
2. Pertussis
3. Herpes simplex infection
4. Metabolic pathways
5. Cell cycle
6. p53 signaling pathway
7. Chagas disease
8. Hypertrophic cardiomyopathy
9. Toxoplasmosis
10. Hepatitis C
11. Leishmaniasis
12. Measles
13. Type I diabetes mellitus
14. MAPK signaling pathway
15. Oocyte meiosis
16. Dilated cardiomyopathy

D **GO analysis, top changed**

1. Negative regulation of cell proliferation
2. Response to virus
3. Response to organic cyclic compound
4. Response to hypoxia
5. Cellular response to organic cyclic compound
6. Negative regulation of gene expression
7. Response to drug
8. Cellular response to interferon-beta
9. Negative regulation of apoptotic process
10. Immune response
11. Positive regulation of smooth muscle cell proliferation
12. Regulation of cell growth
13. Innate immune response
14. Cellular response to lipopolysaccharide
15. Inflammatory response
16. Cellular response to hypoxia

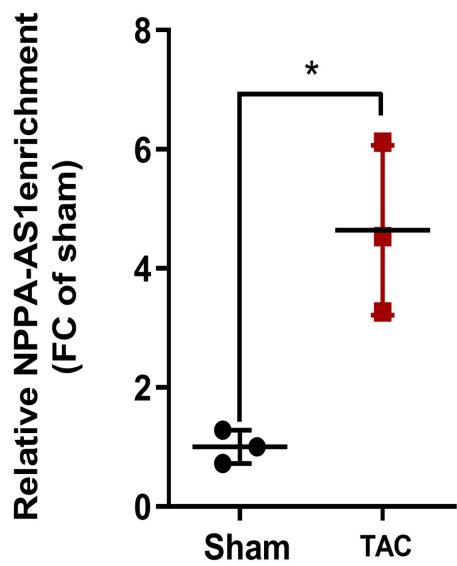
A1**A2****A3****A4****A5****B**

Supplementary Figure S6

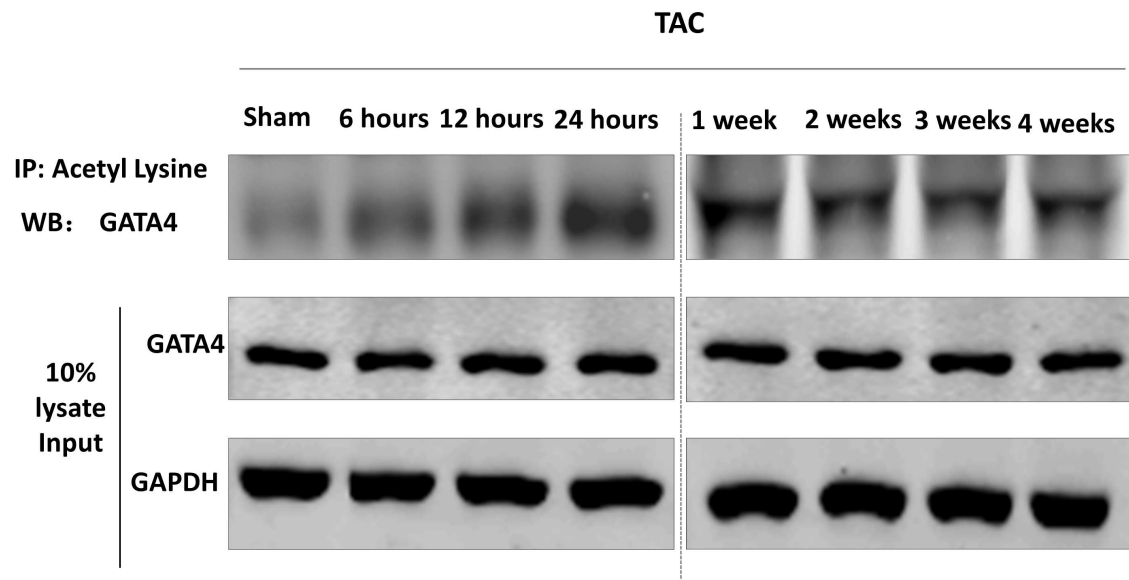


Supplementary Figure S7

A

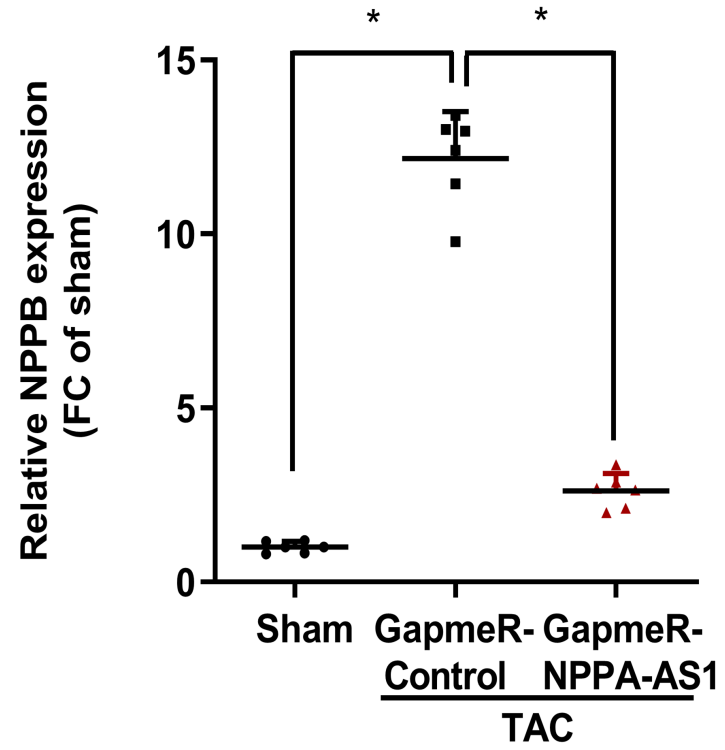


B

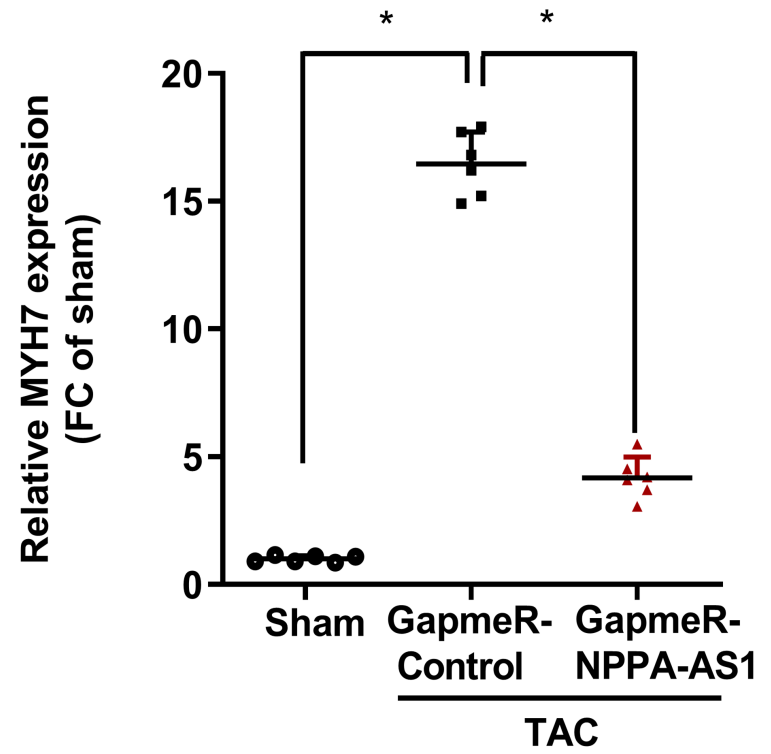


Supplementary Figure S8

A



B



Supplementary Figure S9

Supplementary Figure legends:

Figure S1 (Related to Figure 1). NPPA-AS1 is a conserved, hypertrophy-associated, non-coding antisense transcript with low coding potential, mainly distributed in cardiomyocyte in heart

NPPA-AS1 expression in different human tissues; data are from RNA seq file of UCSC website (<https://genome.ucsc.edu/>). (B) NPPA-AS1 expression in different mouse tissues, data are from NONCODE website (<http://www.noncode.org/>). (C) Mouse NPPA-AS1 expression in different tissues, validated by real-time qPCR. *P < 0.05 versus heart, one-way ANOVA, Holm-Sidak test (n = 6). (D) NPPA-AS1 expression is significantly increased in serum of cardiac hypertrophy patient. RNAs isolated from serum of healthy controls (Control), hypertensive patients (Hypertension), and patients with cardiac hypertrophy (Hypertrophy), were subjected to real-time qPCR to detect NPPA-AS1 expression levels, n = 103 for control groups, n = 101 for hypertension group, n = 92 for hypertrophy groups. Data are mean \pm SD. *P < 0.05 vs Control, one-way ANOVA, Holm-Sidak test. (E) Coding potential score of coding and non-coding genes. Related RNA sequences were subjected to Coding potential calculator (CPC, http://cpc.cbi.pku.edu.cn/programs/run_cpc.jsp) to predict the coding potential. (F) Coding probability of coding and non-coding genes. Related RNA sequences were subjected to coding potential assessment tool (CPAT, <http://lilab.research.bcm.edu/cpat/>) to predict the coding probability. (G) NPPA-AS1 is an antisense transcript with high conservation among rodents and other species. Schematic illustration of NPPA-AS1 RNA originating from the antisense of NPPA and the conservation of NPPA-AS1, by blasting in UCSC website (<https://genome.ucsc.edu/>). (H) NPPA-AS1 mainly distributed in cardiomyocyte in heart. RNA fluorescence in situ hybridization was performed to detect NPPA-AS1 distribution in cell types other than cardiomyocytes in the heart. Fibroblasts were stained with collagen I, endothelial cells were stained with CD31, smooth muscle cells were stained with α -SMA, epicardial progenitor cells were stained with Tbx18, and macrophages were stained with CD11b.

Figure S2. NPPA-AS1 modulates cardiomyocyte hypertrophy in vitro.

(A) Knock-down efficiency of NPPA-AS1 ASO in rat neonatal cardiomyocytes. ASO was designed to knock down rat NPPA-AS1 in neonatal cardiomyocytes, with or without phenylephrine (PE 10 μ M, 48 h) stress (n = 3). Rat cardiomyocytes, instead of mouse cardiomyocytes, were used because mouse cardiomyocytes do not respond well to PE stimulation; mouse and rat lncRNAs have homologous sequences (Figure 1G). The expression of NPPA-AS1 was quantified by real-time qPCR. Data are mean fold-change (FC) relative to scramble \pm SD. *P < 0.05 vs. scramble, one-way ANOVA, Holm-Sidak test. (B) Effect of knocking down of NPPA-AS1 expression on cell size under PE stress. Neonatal rat ventricular myocytes (NRVMs) were transfected with NPPA-AS1 ASO or scramble ASO (n = 3), treated with PE (10 μ M, 48 h). Control NRVMs were treated with vehicle (bars, 50 μ m). Cell size was calculated using image G. Data are mean fold-change (FC) relative to scramble \pm SD. Red: α -actinin, Blue: DAPI. *P < 0.05 vs. PE, one-way ANOVA, Holm-Sidak test. (C) Effect of block NPPA-AS1 on expression of fetal genes NPPB and MYH7 under PE stress.. (n = 3). *P < 0.05 vs. PE, one-way ANOVA, Holm-Sidak test. (D) Over-expression efficiency of NPPA-AS1 in NRVMs (n = 3). (E) Effect of NPPA-AS1 over expression (OE) on size of NRVMs (bars, 50 μ m). (n = 3). Data are mean fold-change (FC) relative to pcDNA3.1 \pm SD. *P < 0.05 versus pcDNA3.1, Student's t-test. (F)

Effect of NPPA-AS1 over expression (OE) on fetal genes MYH7 expression in NRVMs (n = 3). Data are mean fold-change (FC) relative to pcDNA3.1 \pm SD. *P < 0.05 versus pcDNA3.1, Student's t-test.

Figure S3 (Related to Figure 2). NPPA-AS1 is required for pressure overload-induced cardiac hypertrophy and remodeling.

(A1) Primers used to detect the expression of different sequences of NPPA-AS1, targeting exon 1 or exon 3, by real-time qPCR. (A2) Exon 1 or exon 3 of NPPA-AS1 expression (real-time qPCR) in WT or NPPA-AS1-inactivated mouse hearts. Data are mean fold-change (FC) relative to WT \pm SD (n = 6/group). *P < 0.05 vs WT, two way ANOVA, Holm-Sidak test. (B) Inactivating NPPA-AS1 had no effect on body development of mice. WT and NPPA-AS1-inactivated mice were examined for body shape and x-ray at 8 weeks of age. (C-D) Heart morphology and heart weight/body weight ratio in WT and NPPA-AS1- inactivated mice at 8 weeks of age (bars, 5 mm). (n = 6/group). (E) Cardiac function of WT and NPPA-AS1- inactivated mice at 8 weeks of age, were tested using echocardiography (n = 6/group). EF = left ventricular ejection fraction, FS = fractional shortening, LVIDd = left ventricular internal dimension at diastole. (F) Reprogramming of fetal genes in WT or NPPA-AS1- inactivated mouse hearts after TAC, expression determined by real-time qPCR, n = 6/group. Data are mean FC relative to WT sham \pm SD. WT: wild-type, *P < 0.05 vs WT, one-way ANOVA, Holm-Sidak test.

Figure S4. Global knockdown of NPPA-AS1 by shRNA mitigated heart remodeling in vivo.

(A) Overview of the experimental setup. 1-day-old mice were intraperitoneal injection of AAV9 sh NPPA-AS1 or control negative (NC) shRNA. TAC was performed when the mice were 8-week-old. The hearts were removed 6 weeks after TAC. (B) NPPA-AS1 expression in NC- or sh NPPA-AS1-injected mouse hearts (n = 3), 6 weeks after sham or TAC, was quantified by real-time qPCR. Data are mean fold-change (FC) relative to NC sham \pm SD. (C) NC and sh NPPA-AS1 AAV-9 intraperitoneal injected mice were examined for body shape and x-ray at 8 weeks of age. (D) Heart morphology in NC and sh NPPA-AS1-injected mice at 8 weeks of age (bars, 5 mm). (E) Heart weight/body weight ratio of NC and sh NPPA-AS1-injected mice (n = 6). Data are mean \pm SD. (F) Gross morphology (bars, 5 mm), histological analysis using hematoxylin and eosin staining (bars, 2 mm), transverse sections analysis using wheat germ agglutinin staining (bars, 20 μ m) and fibrosis analysis using masson trichrome staining (bars, 500 μ m), of adult hearts from NC- and sh NPPA-AS1-injected mice after TAC or sham. (G) Quantification of the size of cardiomyocytes by measurement of transverse cell area, Data are mean fold-change (FC) relative to NC sham \pm SD. (n = 6). (H) Quantification of the stained fibrosis area, Data are mean fold-change (FC) relative to NC sham \pm SD. (n = 6). (I) Echocardiographic analyses of cardiac function of adult hearts from NC- and sh NPPA-AS1-injected mice 6 weeks after TAC or sham (n = 6). Data are mean \pm SD. (J) Reprogramming of fetal genes, NPPB and MYH7, quantified by real-time qPCR in NC- and sh NPPA-AS1-injected mouse hearts (n = 6). Data are mean FC relative to NC sham \pm SD. EF = left ventricular ejection fraction; FS = fractional shortening; LVIDd = left ventricular internal dimension at diastole. LVIDs = left ventricular internal dimension at systole. LVPWd = Left ventricular posterior wall at diastole; IVSd = Interventricular septal at diastole. *P < 0.05, two-way ANOVA, Holm-Sidak test.

Figure S5. Cluster of genes regulated by NPPA-AS1.

(A-B) Transcriptome microarray was performed with hierarchical clustering and volcano plot analyses of different expressed genes in NPPA-AS1 knock-down NRVMs, relative to scramble. Both samples were treated with PE (10 μ M, 48 h). (C-D) Gene ontology and pathway analyses of unregulated genes and the top 16 in the most-changed list.

Figure S6 (Related to Figure 3). Predicted interaction and validation of NPPA-AS1 RNA and candidate transcription factors.

(A) Predicted interaction of NPPA-AS1 RNA (nucleotide positions) and candidate transcription factors (amino acid residues), included GATA6, MEF2C, NKX2-5, FOXO3A and HIF1A. (B) Validation of interaction of NPPA-AS1 and candidate transcription factors. Representative Chromatin isolation by RNA purification (ChIRP) assay was used to detect interaction of above transcription factors with NPPA-AS1 probe or LacZ probe in mouse cardiomyocytes. LacZ probe was set as negative control. Associated proteins were detected by western blotting.

Figure S7 (Related to Figure 4). NPPA-AS1 regulates the GATA4-dependent transcription of target genes.

(A) Hierarchical clustering analyses of un-regulated genes from GATA4 ChIP-Seq in vehicle and phenylephrine (PE) induced NRVMs. PE (10 μ M, 48 h) treated NRVMs were transfected with NPPA-AS1 siRNA or scramble. (B) Pathway analysis of up-regulated genes in PE stressed NRVMs compared with vehicle treated NRVMs. (C) Pathway analysis of down-regulated genes in NPPA-AS1 knock-down NRVMs compared with PE treated NRVMs. (D) Visualization of GATA4 ChIP-seq and NPPA-AS1 ChIP-Seq data tracks. Cardiac hypertrophy and remodeling related genes were selected and IGV screen shots was used to show representative peaks, included AKT1, C-jun, C-fos, MAPK1, MAPK11, NFATC1, NFATC3 and SRF. (E-F) Effect of si NPPA-AS1 on GATA4-dependent transcription of target genes. (E) Target genes expression regulated by GATA4 were quantified by real-time qPCR (n = 3). Cardiomyocytes were separately co-transfected with pcDNA3.1 vector, NPPA-AS1 siRNA, GATA4, alone or in combination. NPPB, MYH7, and endothelin-1(EDN1) expressions were detected 48 hours after co-transfection. (F) Dual-luciferase reporter gene assays were performed to test the promoter activity of NPPB, MYH7, and EDN1 (n = 3). Cardiomyocytes were separately co-transfected with pcDNA3.1 vector, NPPA-AS1 siRNA, GATA4, pGL3-basic, pGL3-NPPB promoter, pGL3-MYH7 promoter, or pGL3- EDN1 promoter plasmids. Relative luciferase activity was tested 48 hours after co-transfection. pRL Renilla luciferase plasmid was also co-transfected to normalize transfection efficiency. Data are mean fold-change (FC) relative to pcDNA3.1 \pm SD. *P < 0.05, one-way ANOVA, Holm-Sidak test.

Figure S8 (Related to Figure 5). NPPA-AS1 is the effector of GATA4 acetylation during cardiac hypertrophy.

(A) NPPA-AS1 enriched on GATA4 during cardiac hypertrophy. RNA immunoprecipitation experiments were performed using GATA4 antibody to incubate with lysates of mouse hearts of sham or TAC 1 week. The enrichment of pulled-down NPPA-AS1 was detected by real-time qPCR. The quantification of both samples are mean percentage of input. Data are mean relative to sham \pm SD. N = 3. (B) Dynamic changes of GATA4 acetylation in hearts during cardiac hypertrophy. Co-IP assays were performed to detect the acetylation of GATA4. Adult mice were

respectively subjected with TAC surgery for 6, 12 or 24 hours and 1, 2, 3 or 4 weeks. The heart tissue lysates were co-incubated with acetyl lysine antibodies. Associated proteins were detected using GATA4 antibodies. 10% lysate were detected using GATA4 or GAPDH antibodies as input. N = 3. *P < 0.05, vs sham, Student' s t-test.

Figure S9 (Related to Figure 6). Pharmacological inhibition of NPPA-AS1 in vivo prevents cardiac hypertrophy and remodeling.

(A-C) Adult mice were subjected to TAC or sham surgery for 6 weeks, with six weekly injections of GapmeR-control (scrambled sequence) or GapmeR-NPPA-AS1, starting at day 1 after TAC until removal of the heart. Removed hearts were used to test reprogramming of fetal genes, NPPA, NPPB, and MYH7. Fetal genes expression were determined by real-time qPCR (n = 6). Data are mean FC relative to sham \pm SD. *P < 0.05, one-way ANOVA, Holm-Sidak test.

1 **Supplemental data:**

2 Mouse NPPA-AS1 full-length sequence:

3 TAAGCCGTGGACCCCTCCACCCATGGCAGTCCCTTCGAACTAGTGGCTCAGTCTCTTAC
4 TTGTCGAAGCTTGGTCCCCACCCCATCCCCAATGCACCACAGCACCTTGTCAGACA
5 CAGTTCCATGGGGGGTCACTGAGGTTGGCTTGAGGCAGTTTCCTGGCTGGCTTCTGCG
6 CCTGGGCATTTGTGTGGCTCCGGTACTGCTGTGGGAGTTGGGTATTTTATGAGATGTCT
7 GCATGTGACCTTGTTAAGCAGTTCAGCTGGGACGGACATTAGCTTGACTCAGCTAGC
8 CATGTGACAGTTTGATGCAGACCTTGGTGACAAGAAAGCTTCCGGAGAGGCCAGCCC
9 AGCCTTCCTGGCCAGCCATGTTGACAAGGAGAGTTGCCCTTGGCTCCTGTGGACCTC
10 AGAGACTGTCCAGTTGCAGCTTCCGCCTTTCGGTCATACTGTGTTTATACGGTAAACATT
11 AGCTGATTCCACTGTGTAGATAAATGGTATCTTTTTTAATTTGTAAGAGTCTATTTTTATT
12 TGGCCCTTTGGAAGGTGGACGTTCTTGTGGTCACTCTTAAGTCAGAATAAAAATGTCT
13 GCACCTTCTCTGTAGACCTTGTCTCCACGGTGCTCGCTCGCTCTTAAGTAGGGAAAGTT
14 AAGGCGCTGTAGCAAAGCAGTCTGTTTCTAAGACAAGGTCTGATGGAACGCAGGCGA
15 TGACCTGAGCTGCCCTGCCCTCCGTACCTTCCACATGCTGGGATTCCAGGTCTCTGCC
16 ATCAGACCCAGCCAGGAAAGGCAGTCTGCTGGCCCGCACCTCCCTTTCAGTGCCTGTC
17 CCCACCCCTCTTTCTTCTGCGGCACCTGTCACCTATGCACACTTTTGGTCTGTTGATCTT
18 TTCTTCCTGCCAGCTGCACCAGGGCAACAGTGGACAGTCTGTCTGGGGACTTACCCCA
19 GAGACGAGAGCCTAACAGCAGCCTGAGGAGAGGAAGCCCTCCAGCTCTCCTGGGTG
20 AGGATCTACCTTAATATGCAGAGTGGGAGAGGCAAGACCCCACTAGACCACTCATCTA
21 CATTAAACATCGATCGTGATAGATGAAGGCAGGAAGCCGCAGCTCCAGGAGGGTGTTT
22 ACCACGCCACAGTGGCAATGTGACCAAGCTGCGTGACACACCACAAGGGCTTAGGAT
23 CTTTTGCGATCTGCTCAAGCAGAATCGACTGCCTTTTCCTCCTTGGCTGTTATCTTCGGT
24 ACTACAAAGAGAAAAATATACTGGCTTGATGATCTGCCTTTACTGGGCTAAATTGTTCC
25 ACTTGAACAGCGATCAACTATTTCCACAAGCCACAGTCTAGCCTCTGTGATTAAACCG
26 GCAAGCAAGGCACTGCTCCTCTTACCCGGAAGCTGTTGCAGCCTAGTCCACTCTGGGC
27 TCCAATCCTGTCAATCCTACCCCGAAGCAGCTGGATCTTCGTAGGCTCCGAGGGCCA
28 GCGAGCAGAGCCCTCAGTTTGCTTTTCAAGAGGGCAGATCTATCGGAGGGGTCCAGG
29 GGCTGCGCCCTAGAGCACTGCCGTCTCTCAGAGGTGGGTTGACCTCCCCAGTCCAGGG
30 AGGCACCTCGGGGAGGGAGCTAAGTGCGGCCCTGCTTCCCTCAGTCTGCTCACTCAGG
31 GCCTGCGGGGCATGACCTCATCTTCTACCGCATCTTCTCCTCCAGGTGGTCTAGCAG
32 GTTCTTTATAAAGGCAAATAAATACAGAGAAAGGGGACGTCTCAGGAATGGACCCAG
33 TACCAA

34

35 NPPA-AS1 rat homologous sequence:

36 GGGTGAGGATCTACCTTAATATGCAGAGTGGGAGAGGTAAGGCCTCACTAAACCACTC
37 ATCTACACTTAACATCGATCGTGATAGATGAAGACAGGAAGCTGCAGCTCCAGGAGGG
38 TATTCACCACCTCTCAGTGGCAATGCGACCAAGCTGTGTGACACACCGCAAGGGCTTG
39 GGATCTTTTGCATCTGCTCGAGCAGATTTGGCTGTTATCTTCGGTACTACAAAGAGAA
40 AAATAAATCGGTCTGATGATCTACCTTCACTGGGCTAACCTCTTACCCGGAAGCTGTTG
41 CAGCCTAGTCCGCTCTGGGCTCCAATCCTGTCAATCCTACCCCGAAGCAGCTTGACCT
42 TCGCAGGCTCCGAGGGCCAGCGAGCAGAGCCCTCAGTTTGCTTTTCAAGAGGGCAGA
43 TCTATCGGAGGGGTCCAGGGGCCGCGCCCGAGAGCACCTCCATCTCTCTGAGACGGG
44 TTGACTTCCCCAGTCCAGGGAGGCACCTCAGAGAGGGAGCTAAGTGCCGCCCCCGCT

1 TCATCGGTCTGCTCGCTCAGGGCCTGCGGAGGCATGACCTCATCTTCTAC
2
3 NPPA-AS1 human homologous sequence:
4 CATTTCCTTAAGTTTTGATCTCCGTCTTCTGATGAAGCAGGCAGAGCTCAGAGGATCT
5 TGGCATCACCCACCAAAGTTAGCTGAAAGCAGGGCACTCCTGGATAAAGCAGCTTAC
6 TCAACTCTGGGGAATGCTACCATTTTTTTTCCAAAGTAGAAAGGAAGCACTTCTGAGC
7 CAGTGACCACTGAAAGATGAACACTCTTCTGATCCTCTCCTCTAGAATTCATCTCCTC
8 CTGCTAGCAGCCGCGTCTGGAGGAGCAGCGGATGGGGAATCCATTCTGTTTCTTCTCCT
9 GGTGTTTAGGAAGTTGCCCCACACACAGATTGCCCGATGTCCAACCAGAAGAAGTGA
10 AACTGCTGCTGGGTCTGGAGAGGTGAAGACCCGTGGCCAGCTTCTGTTGTTGCCATCG
11 GCCATTGCTTTTTGTTTCGCTTGCTTTTGGTTTTGCAAGAAGAGCGGCCTCTGTCTCTGA
12 TCTGCTTCAAATCATCATTCCATCAGTGACAGAAGTGGCTGTTCCATCAGTGGTTCGCAG
13 CCAGTTCAGCTCCTGCATCCATCCCCAAGTGTCTGAGTGGAAATTTGAGGCCTCCCCAA
14 CCACCTACCAAAAAAGGAGGGTGAATGAAAGGAAGAAGAAAAACTCAGCATTCTTT
15 CCTCTGACAAAGAGTAAAACGACAAGGAATATCGGCCTGAATTCTCTTCCCAAGAAGA
16 AAGAAAGCACACCAACGCAGGCATTTGTCTTCTGTCCATGGTGCTGAAGTTTATTCACT
17 TTCAAACCACTTTTCAGTAACAGCAAATTTCTTTAGAAAAGGAAAATACAGGGAAAGGGA
18 TAAACCTCACTGACTTGGAGGAAATCAAGAGGAGTGAGCACAGCATCAGAAAGCCCC
19 CTGGCCCCAGACTGCACCCGCTTTCCTGGCCCTACCTTGAAATCCATCAGGTCTGCGTT
20 GGACACGGCATTGTACATGGGATTAGCTCTGGTCTGACCTAGGAGCTGGAATGCCAGT
21 AAAAGGAGGAAGCTCACGGTGGTGGTGGAGAAGGAGCTCAT

22
23

24 **Supplemental Table 1: General characteristics of participants:**

25

	Control (n=103)	Hypertension (n=101)	Hypertrophy (n=92)	P-value
Age (year)	66.53±12.55	66.68±10.22	68.46±10.75	0.424
Sex (M/F)	50/53	49/52	51/41	0.542
Systolic blood pressure (mm Hg)	112.12±12.23	163.82±15.34	161.15±13.27	<0.0001
Diastolic blood pressure (mm Hg)	70.23±8.91	94.21±10.64	93.68±9.74	<0.0001

26 Data are presented as mean ± SD. One-way ANOVA, Holm-Sidak test was used for statistical
27 analysis. Chi-square test was used for sex-related statistical analysis.

28
29
30
31

1 **Supplemental Table 2: Primers list:**

2

Gene	Forward Primer	Reverse Primer
r-NPPA-AS1	GGCTAACCTCTTACCC GGAA	CTGGGACCCCTCCGATAGA T
r-NPPA	TGAGCCGAGACAGCA AACAT	CAATATGGCCTGGGAGCCA A
r-NPPB	CAGAAGCTGCTGGAG CTGATA	GGCGCTGTCTTGAGACCTA A
r-MYH7	CCGAGTCCCAGGTCA ACAAG	CTTGGAGCTGGGTAGCACA A
r-EDN1	TTTGAAGACCGCGCT GAGAT	TGCAAAACGAAGAGGACG GT
r-GAPDH	GCCCAGCAAGGATAC TGAGA	GATGGTATTCGAGAGAAGG GAGG
m-NPPA-AS1	TTGATCTTTTCTTCCTG CCAGC	TTAGGCTCTCGTCTCTGGG G
m-NPPA-AS1 exon1	AGGGAAAGTTAAGGC GCTGT	CAGCATGTGGAAGGTACGG A
m-NPPA-AS1 exon3	TCTCCTCCAGGTGGTC TAGC	CTGGGTCCATTCTGAGAC G
m-NPPA	ATTGACAGGATTGGAG CCCA	CACAGTGGCAATGTGACCA A
m-NPPB	AGTCCTAGCCAGTCTC CAGA	CTTTTGTGAGGCCTTGGTC C
m-MYH7	CAGACATAGAGACCTA CCTTC	CAGCATGTCTAGAAGCTCA GG
m-GAPDH	CCACTCTTCCACCTTC GATG	CCACCACCCTGTTGCTGT A
m-Neat1	ACCCTTTTTTCATGGGG	GCTGGATGGAGGCTTGTTT

	GTAG	A
m-18S	CGCGGTTCTATTTTGT TGGT	AGTCGGCATCGTTTATGGTC
m-Fendrr	CTGCCC GTGTGGTTAT AATG	TGACTCTCAAGTGGGTGCT G
m-snoRNA	CAGAGTAGCGAGGAC TTGAAGAG	GCTGGTTCGTCTATCTTGTG GG
m-NFAT	CCAGATCACAGCACA CGGT	CGATCGGTTCTTCTCGGTC C
m-CREB	GAGAAGCGGAGTGTT GGTGA	CCGGATCTCGCTGGAGTTT T
m-NFAT	CAGATCACAGCACAC GGTCC	TGTGCGATCGGTTCTTCTC G
m-GATA4	AGCAGGACTCTTGGA ACAGC	GCCCCAGCCTTTTACTTTGC
m-Hif1a	GCGAGAACGAGAAGA AAAAGATGA	GAGCTCACATTGTGGGGAA GT
h- NPPA	CCCATGTACAATGCCG TGTC	GGGCACGACCTCATCTTCT A
h-NPPA-AS1 (Real-time PCR)	TCCTGGATAAAGCAGC TTCAC	AGTGTTTCATCTTTCAGTGG TCAC
h-GAPDH	AATGGGCAGCCGTTA GGAAA	AGGAGAAATCGGGCCAGCT A
h-NPPA-AS1 (Droplet-digital PCR)	TCCTGGATAAAGCAGC TTCAC	AGTGTTTCATCTTTCAGTGG TCAC
h-NPPA-AS1 (Probe for droplet-digital PCR)	AAAGTAGAAAGGAAGCACTTCTGAGCC	

1
2

1 **Materials and methods**

2 **Human serum samples**

3 The human serum samples were obtained from patients treated at the Department of Cardiology,
4 Daping Hospital, The Third Military Medical University, Chongqing, China. Exclusion criteria
5 included tumor and renal insufficiency [$GFR < 60 \text{ ml}/(\text{min} \cdot 1.73 \text{ m}^2)$]. From June 2018 to June 2020,
6 400 eligible inpatients, 18 to 95 years of age, were recruited. 296 age- and sex-matched volunteers
7 were divided into control, hypertension, and cardiac hypertrophy groups. Cardiac hypertrophy
8 patients were diagnosed through transthoracic echocardiography, according to the 2011 guidelines
9 of the American Society of Echocardiography (ASE). Patients with hypertension were diagnosed
10 based on the criteria, systolic blood pressure ≥ 140 mmHg and/or diastolic blood pressure ≥ 90
11 mmHg without medication, according to the 2018 Chinese guidelines for prevention and treatment
12 of hypertension. Control patients were those who with normal blood pressure, and were suspected
13 of coronary heart disease but ultimately "ruled out" after coronary angiography. The analysis of
14 human serum samples was approved by the Ethical Committee of The Third Military Medical
15 University, Chongqing, China, and written; informed consents were obtained from the patients and
16 families of the donors. The serum samples were frozen immediately after they were obtained and
17 stored in liquid nitrogen, until further use.

18 **Human heart samples**

19 The human heart tissues were provided by Professor Qizhu Tang from Renmin Hospital, Wuhan
20 University, Wuhan, China. Analysis of human heart tissues was permitted by the Ethical
21 Committee of Renmin Hospital, Wuhan University, Wuhan, China, and the Ethics Committee of
22 The Third Military Medical University, Chongqing, China, and written-informed consents were
23 obtained from the patients and families of the donors. Samples of failing hearts were from HCM
24 patients undergoing cardiac transplantation and control hearts were from healthy hearts that did
25 not meet the transplant standard. Heart samples were frozen immediately after they were obtained
26 and stored in liquid nitrogen, until further use.

27 **Animal experiments**

28 All animal experiments were approved by the Animal Care and Use Committee of the Third
29 Military Medical University, according to the State Science and Technology Commission
30 Regulations for the Administration of Affairs Concerning Experimental Animals and were
31 conducted according to the approved protocols. Transverse aortic constriction (TAC) was
32 performed on C57BL/6J mice (8-10 weeks old) to establish a cardiac hypertrophy model, as
33 described previously¹. Briefly, after the mice were anesthetized with isoflurane (rapid anesthesia
34 with 2.5%–3.5% and maintained with 1.5%–2% isoflurane), TAC was performed. The ascending
35 aorta was ligated between the origins of the right and left carotid arteries, using a 7-0 nylon suture
36 against a 26-gauge needle that is parallel to the transverse aorta. Sham operation involved thoracic
37 incision and aortic dissection but without ligation of the aorta. For global knockdown of
38 NPPA-AS1 expression, AAV9 sh NPPA-AS1 or control negative (NC) shRNA were
39 intraperitoneally injected in one-day-old mice. TAC was performed when the mice were 8 weeks
40 old. Hearts of mice were harvested for analysis at 8 weeks of age at basal state or at 6 weeks after
41 TAC. GapmeR-NPPA-AS1 or related GapmeR-negative control (20 mg/kg) (both from Exiqon) in
42 saline (0.9% NaCl) as the carrying medium was administered weekly by intraperitoneal injection,
43 as described previously².

44 **Generation of transgenic mice**

1 To achieve inactivation of NPPA-AS1 *in vivo*, CRISPR–Cas9 editing approach was used. 3*
2 poly A premature termination signal sequence was inserted behind Exon 1 of mouse NPPA-AS1 to
3 create premature termination, inhibiting transcription of Exon 2 and Exon 3 of the NPPA-AS1,
4 without disturbing the core transcriptional regulatory elements of NPPA gene on the antisense
5 strand. The donor DNA, as repairing template, was generated by combining an N-terminal nuclear
6 localization signal fused GFP (NLS-GFP). GFP was inserted in front of poly A to trace the
7 inserted sequence. LoxP was also used for removing inserted DNA sequence in further studies.

8 **Echocardiography**

9 Transthoracic ultrasonography was performed with a linear 30MHz transducer Vevo 2100
10 system (Fuji Film Visual Sonics, Ontario, Canada) in mice at the indicated time point after TAC.
11 The mice were sedated by inhalation of isoflurane and oxygen (1.3% and 98.7%, respectively),
12 kept their heart rate at 450–550 beats/min, and placed them on a heating blanket to maintain body
13 temperature at 37°C. Measurements were obtained with M-mode tracings and the hearts were
14 viewed at the mid papillary muscle level. All measurements were done for at least 4 cardiac cycles
15 and averaged; chamber size, wall thickness, interventricular septal thickness, fractional shortening,
16 and left ventricular internal dimensions at diastole and systole were obtained.

17 **Cardiomyocyte isolation and culture**

18 Ventricular myocytes were isolated from 1-2-day-old Sprague-Dawley rats or mice, as
19 described previously³. Briefly, a thoracotomy was performed after euthanasia of neonatal rats or
20 mice. The hearts were removed immediately and then washed in ice-cold sodium bicarbonate-,
21 Ca²⁺-, and Mg²⁺-free Hanks balanced salt solution (D-Hanks). The hearts were minced, and the
22 minced tissues were dispersed in a series of incubations at 37°C with 1.25 mg/mL trypsin (Difco)
23 and 0.08 mg/mL collagenase (Worthington). The dissociated cells were aspirated by sterile plastic
24 pipettes and new medium without trypsin and collagenase was added to stop the digestion. The
25 cells were harvested by centrifugation at 1000 g, and the cells were re-suspended in DMEM
26 medium (Gibco) containing 10% FBS (Gibco), penicillin/streptomycin and 0.1 mM Brdu. The
27 cells were plated in culture dishes for 2 hours to remove fast-adherent fibroblasts and then
28 ventricular myocytes were collected and plated in new culture dishes or coverslips coated with
29 laminin. After 48 hours, the culture medium was replaced with serum-free DMEM. The cells
30 were treated with phenylephrine (10 μM, 48 hours) after starvation for 24 hours and various
31 treatments, including cell transfections were performed.

32 **Isolation and culture of epicardial progenitor cell and cardiac fibroblast**

33 Six-well plates coated with 1% gelatin were used for the isolation of epicardial progenitor cell,
34 as previously described⁴. Briefly, hearts of E11.5 mice were dissected, and the vascular tissues
35 were removed with forceps. The right ventricle was excised and sliced; the slices were placed into
36 plates and covered with sterile coverslips. The ventricle samples were cultured in humidified
37 atmosphere with 5% CO₂ at 37°C with Dulbecco's modified Eagle's medium (DMEM), containing
38 10% fetal bovine serum, 100 μg/ml streptomycin, and 100 units/ml penicillin. After 24 hours, the
39 ventricle was removed with forceps when epicardial progenitor cells migrated from the edge of the
40 ventricle onto the plates. Then the cells were cultured for another 24 hours and fixed with 4%
41 paraformaldehyde for 10 min. For isolation and culture of cardiac fibroblasts, 1–3-day-old
42 Sprague–Dawley rats were used, as previously described⁵. In brief, hearts of newborn rats were
43 removed, cut in pieces, and digested with collagenase and trypsin. Cell suspensions were
44 centrifuged at 1000 g for 5 min and the cell pellets were resuspended with DMEM containing 10%

1 fetal bovine serum, 100 µg/ml streptomycin, and 100 units/ml penicillin. Then, the cells were
2 plated for 2 hours in humidified atmosphere with 5% CO₂ at 37°C to allow fibroblast attachment
3 to the culture plates. Afterwards, the non-attached cardiomyocytes were removed, and the attached
4 cardiac fibroblasts were further cultured for 12 hours followed, by fixation with 4%
5 paraformaldehyde for 10 min.

6 **Cell immunostaining**

7 Immunostaining was essentially performed, as described previously ⁶. After washing the
8 cardiomyocytes with PBS, they were fixed with 4% paraformaldehyde for 20 min at room
9 temperature. After removing the paraformaldehyde by straw, the cardiomyocytes were treated with
10 0.1% Triton-X 100 dissolved in PBS for 10 min, followed by incubation with immunostaining
11 blocking solution (Byotime, China) for 20 min. The cardiomyocytes were washed three times with
12 PBS and then incubated with primary antibody against tropomyosin (Sigma) at 4°C overnight,
13 followed by incubation with fluorescence-conjugated secondary antibody.

14 **RNA isolation and real-time qPCR**

15 RNA was isolated from tissues and cells, using Trizol Reagent (TAKARA, Japan). RNA was
16 reverse-transcribed into first-strand cDNA by one-step First Strand cDNA Synthesis Kit
17 (TAKARA, Japan). RNAs isolated from 48 hours after plasmid transfected cell were pre-treated
18 with DNase to remove remaining plasmid template, before reverse-transcription into cDNA. RNA
19 isolation from human serum was performed using miRNeasy Serum/Plasma Kit (QIAGEN,
20 Germany), following the manufacturer's instructions. Real-time qPCR was performed using
21 SYBR Green dye (TAKARA, Japan) that was detected by CFX96 Real-Time PCR Detection
22 System (Bio-Rad, CA). Gene expression was normalized by GAPDH to calculate relative
23 expression levels. The PCR primers are listed in the **Supplemental Table 2**.

24 **Histological analysis**

25 The hearts from all groups were washed in PBS and fixed in 4% paraformaldehyde at 4°C
26 overnight, embedded in paraffin, and sectioned into 5 µm-thick slices. The heart sections were
27 stained with hematoxylin and eosin (HE) to measure the thickness of the heart wall and heart size.
28 To measure cardiomyocyte dimensions, the cardiomyocytes were stained with FITC-conjugated
29 wheat-germ agglutinin (FITC-WGA, Sigma Aldrich) and the nuclei stained with 4',
30 6-diamidino-2-phenylindole (DAPI, Byotime, China). To assess fibrosis, the heart sections were
31 stained with Masson trichrome kit (ZhongShanJinQiao, China). The size of the cardiomyocytes
32 and amount of fibrosis of the hearts were calculated by Image J software.

33 **Plasmid Constructs**

34 Plasmid GATA4 consisted of mouse GATA4 full-length cDNA. For luciferase assay, the
35 reporter plasmids pNPPB-luc, pMYH7-luc, and pEDN1-luc were driven by a 2000-bp of mouse
36 NPPB, MYH7, and EDN1 promoter sequence. The luciferase control reporter vectors were
37 Promega pRL Renilla luciferase reporter vectors.

38 **RNA immunoprecipitation (RIP)**

39 RNA-protein interactions were validated by RIP, as described previously ⁶, using the Magna
40 RIP RNA-Binding Protein Immunoprecipitation Kit (17-701, Millipore). GATA4 antibody was
41 used for immunoprecipitation, with mouse IgG, as negative control. In brief, 1-2×10⁷ mouse
42 cardiomyocytes were homogenized in adequate volumes of lysis buffer, which included protease
43 inhibitor cocktail and RNase inhibitor for protein and RNA protection. The homogenized
44 cardiomyocytes were centrifuged at 14,000 g for 10 min at 4°C to remove cell debris. Protein A/G

1 beads were washed using RIP wash buffer and 5 μ g GATA4 antibody were added. Beads and
2 antibody were incubated with rotation for 30 min at room temperature and then the supernatant
3 was removed. Beads/antibody and cell lysate complex were incubated, rotating for 3 hours at
4 room temperature, and incubated overnight at 4°C. After incubation, protein in complex was
5 digested by proteinase K buffer and the bound RNAs were extracted by phenol: chloroform:
6 isoamyl alcohol (125:24:1) buffer. Extracted RNAs were reverse-transcribed into first-strand
7 cDNA for detecting the associated RNAs by real-time qPCR; total RNAs from cell lysates were
8 quantified, simultaneously as quality controls (Input).

9 **Western blotting assay**

10 For western blotting, proteins extracted from cells or tissues were electrophoresed on
11 SDS-PAGE and transferred onto nitrocellulose membranes, and then incubated with the following
12 antibodies: EP300 (sc-585X, Santa Cruz, 1:500), GATA4 antibody (Santa Cruz, sc-25310, 1:500),
13 GATA6 (55435-1-AP, Proteintech, 1:500), MEF2C (10056-1-AP, Proteintech, 1:500), FOXO3A
14 (10849-1-AP, Proteintech, 1:500), NKX2-5 (13921-1-AP, Proteintech, 1:500), HIF1A (sc-13515,
15 Santa Cruz, 1:500). Analysis of GATA-4 acetylation was performed as described previously ⁷.
16 Briefly, the cell lysates were incubated with protein A sepharose beads (Invitrogen)/acetyl lysine
17 antibody (ab21623, Abcam, 4 μ g) complex at 4°C overnight. The beads were washed, and the
18 retrieved proteins were detected by GATA4 antibodies.

19 **Co-immunoprecipitation (Co-IP) assay**

20 For co-IP, EP300 antibody and acetyl lysine antibody were the capture antibodies and GATA4
21 was the detection antibody; the amounts of antibodies were both 4 μ g. Analysis of GATA-4
22 acetylation was performed using Co-IP as described previously ⁷. Above antibodies were
23 incubated with cell or tissue lysates at 4°C overnight followed by incubation with protein A
24 sepharose beads (Invitrogen) at room temperature for 2 hours. The beads were washed, and the
25 retrieved proteins were detected by GATA4 antibodies. 10% of cell or tissue lysates were used as
26 input. EP300, GAPDH, and GATA4 antibodies were used to test the loading control of related
27 samples.

28 **Luciferase reporter assay**

29 Luciferase reporter assays were performed using the Promega Dual-Luciferase® Reporter
30 Assay System (E1910) in cardiomyocytes following the manufacturer's instructions. Reporter
31 plasmids, GATA4 overexpression plasmids, NPPA-AS1 siRNA, were co-transfected using
32 lipofectamine 3000 reagent (Invitrogen, Lot No.11668-019). 24 hours after transfection, luciferase
33 activities were measured with a Dual-Luciferase® Reporter Assay System. pRL Renilla luciferase
34 plasmid was also co-transfected to normalize transfection efficiency; the reporter plasmids
35 amounts were pRL Renilla luciferase plasmid = 10:1.

36 **Bioinformatics and statistical analysis**

37 Coding potential calculator (CPC, http://cpc.cbi.pku.edu.cn/programs/run_cpc.jsp) and coding
38 potential assessment tool (CPAT, <http://lilab.research.bcm.edu/cpat/>) were used to analyze
39 NPPA-AS1 coding potential. The protein-RNA binding propensity between NPPA-AS1 fragments
40 and proteins was predicted using catRAPID (http://s.tartagialab.com/page/catrapid_group).
41 Significance Analysis of Microarrays (SAM) was used to test for differential gene expression⁸,
42 Benjamini-Hochberg false discovery rate (FDR) method was used to perform multiple-hypothesis
43 testing, as described previously⁹. KEGG pathway analysis
44 (<http://www.genome.jp/kegg/pathway.html>) and Gene ontology (GO) analysis

1 (<https://david.ncifcrf.gov/>) were used to analyze differentially expressed genes in gene chip.
2 Transcriptional factors of NPPA-AS1 promoter binding were predicted in JASPAR website
3 (http://jaspar.genereg.net/cgi-bin/jaspar_db.pl?rm=browse&db=core&tax_group=vertebrates).

4 **Chromatin Immunoprecipitation-sequencing (ChIP-Seq) and related analysis**

5 ChIP seq was performed using Millipore Magna ChIP™ A - Chromatin Immunoprecipitation
6 Kit (17-371), as described previously^{10,11}. Briefly, 5x10⁷ cardiomyocytes were crosslinked with
7 1% formaldehyde for 10 min at room temperature (RT) and then terminated with 2.5 M glycine at
8 RT for 7 min. After ice-cold PBS rinse, the cells were lysed in SDS lysis buffer containing 1X
9 protease inhibitor cocktail II. Then, EZ-Zyme™ Chromatin Prep Kit (Millipore, 17-375) was used
10 to shear crosslinked DNA to yield 100-1000 base pair DNA fragments. Protein G Agarose beads
11 and cell lysates were co-incubated for 1 hour at 4°C with rotation to remove non-specific binding.
12 Thereafter, the agarose beads were obtained after brief centrifugation. 1% of the samples served as
13 input. Samples were incubated with GATA4 antibody (Santa Cruz, sc-25310) overnight at 4°C
14 with rotation, to precipitate the DNAs. Subsequently, pre-clearing beads were added to each IP and
15 incubated for 1 hour at 4°C with rotation. To elute, reverse crosslinks, digest, and purify the
16 protein/DNA complexes, the samples were washed with a series of buffers including 2% SDS, 0.1
17 M NaHCO₃, high and low salt concentrations, proteinase K digestion solution, and filtered through
18 spin columns. The retrieved ChIP DNAs were then used to construct Illumina sequencing libraries
19 following the NEB Next ChIP-Seq Sample Prep Master Mix Set1 protocol (E6240, NEB). DNA
20 sequencing was performed on an Illumina HiSeq PE150, by the Nuohezhiyuan Company
21 (Tianjing, China). Reads were specifically mapped to reference rat genome. The peak caller
22 program MACS2 was used to identify peaks with the following threshold of q value ≤ 0.05. IGV
23 (Broad Institute, MA) was used to visualize the peaks for selected genomic loci.

24 **Deletion mapping and RNA pull-down assay**

25 Deletion mapping and RNA pull-down assay were performed according to protocols described
26 previously⁷. Briefly, the protein-RNA binding propensity and related interaction positions
27 between NPPA-AS1 and candidate proteins were predicted using catRAPID
28 (http://s.tartagliolab.com/page/catrapid_group). FASTA formats of RNA sequence and protein
29 sequences were loaded into catRAPID fragments website, to analyze the interaction propensity
30 and discriminative power. Based on the prediction results, different lengths of NPPA-AS1
31 fragment were cloned into pcDNA3.1 plasmid vector. To generate biotinylated RNAs, plasmids
32 were used for *in vitro* transcription with the Biotin RNA Labeling Mix (Roche) and T7 RNA
33 polymerase (Promega). Biotin-labeled RNAs from *in vitro* transcription were then treated with
34 DNase I (TAKARA, Japan) and purified using the Mini Quick Spin Column (Roche). Newly
35 synthesized RNAs were heated at 60°C for 10 min and slowly cooled to RT, to facilitate secondary
36 structure formation. Because NPPA-AS1 is mainly located in the nucleus, Nuclear and
37 Cytoplasmic Protein Extraction Kit (Beyotime, China) was used to extract nuclear proteins in
38 5x10⁷ cardiomyocyte cells, with the addition of protease inhibitor Cocktail (Abcam, US). One mg
39 nuclear extracted protein and 50 pmol of synthesized biotin labeled RNAs were mixed in RNA
40 binding buffer. The mixture was incubated in 30°C water bath for 30 min to facilitate RNA-protein
41 complex formation. Pre-washed streptavidin agarose beads (Invitrogen) were further added in
42 each tube and incubated at room temperature for 1 hour with rotation. Beads were washed five
43 times using RNA binding buffer and boiled in protein loading buffer, and captured proteins were
44 analyzed using western blotting.

1 RNA fluorescence in situ hybridization (FISH)

2 RNA FISH was performed according to manufacturer's instructions, using the RiboTM
3 Fluorescence *In Situ* Hybridization Kit (Guangzhou Ribo Biotechnology Company, China).
4 Briefly, cardiomyocytes were fixed with 4% paraformaldehyde for 10 min at RT. After removing
5 the paraformaldehyde by straw, the primary cardiomyocytes, primary fibroblasts, primary
6 epicardial progenitor cells, smooth muscle cells (ATCC, CRL-2797), macrophages (ATCC, TIB-7),
7 and endothelial cells (ATCC, CRL-2581) were treated with 0.5% Triton-X 100 dissolved in PBS
8 for 5 min at 4°C, followed by incubation with primary antibody against tropomyosin (Sigma,
9 T2780), Collagen I (Abcam, ab34710), TBX18 (Abcam, ab115262), α -SMA (Abcam, ab19245),
10 CD11b (BD Bioscience, 557686), or CD31 (Abcam, ab28364) at 4°C overnight, and continuous
11 incubation with fluorescence-conjugated secondary antibody. After immunostaining, the
12 cardiomyocytes were incubated with pre-hybridization buffer for 30 min at 37°C. Then, the probes
13 (0.5 μ M) were mixed with hybridization buffer, including targets of NPPA-AS1, 18s and u6, and
14 incubated at 37°C overnight. Then, the cells were serially incubated with saline sodium citrate
15 buffer I, II, III. The nucleus was stained with DAPI.

16 RNA electrophoretic mobility shift assay (EMSA)

17 RNA EMSA assays were performed as previously published¹². Briefly, RNA probes for
18 NPPA-AS1 were synthesized and labeled with biotin using the RNA 3' End Biotinylation Kit
19 (Thermo Fisher Scientific), according to the manufacturer's protocols. Recombinant EP300 or
20 GATA4 protein was expressed from linearized pT7CFE1-P300 and pT7CFE1-GATA4 (Addgene)
21 respectively in a coupled transcription and translation system (Thermo Fisher Scientific),
22 according to the manufacturer's protocols. Then EMSA was performed using a LightShift
23 Chemiluminescent RNA EMSA Kit (Thermo Fisher Scientific) according to the manufacturer's
24 protocol. 1 μ L out of 20 μ L *in vitro* - translated recombinant protein was incubated with 10 pmol
25 of labeled probe at room temperature for 30 min. Unlabeled probes were used for competitors. The
26 reactions were then separated on a 1% 0.5 \times TBE - agarose gel and transferred to a positively
27 charged nylon membrane (Roche) in the dark. After separation, the membrane was cross-linked by
28 exposure to UV, followed by incubation with HRP-conjugated streptavidin. The membranes were
29 visualized with ECL reagents. The sequences of the RNA probes are listed in **Table 4**.

30 Droplet-digital PCR (ddPCR)

31 Human NPPA-AS1 copy numbers were quantified using a Bio-Rad QX200 Droplet Digital
32 PCR system with ddPCR Supermix for Probes (Bio-Rad), according to the manufacturer's
33 protocols. Briefly, 20 μ L reaction mix consisted of 10 μ L of 2 \times ddPCR Supermix, 1 μ L of
34 forward primer, 1 μ L of reverse primer, 2 μ L of probe, and 6 μ L cDNA template. Then droplet
35 generation for ddPCR was done using the QX200 droplet generator (Bio-Rad), following
36 manufacturer's instructions. After droplet generation, reaction mix was transferred into a 96-well
37 plate, sealed, and cycled in a C1000 Touch thermal cycler (Bio-Rad). The cycling protocol was
38 95°C for 10 min, followed by 39 \times 95°C for 30 s and 60°C for 60 s and 98°C for 10 min. The
39 cycled plates were read by a Bio-Rad QX200 droplet reader, which counts all generated droplets
40 and detects the amount of PCR product-positive (fluorescent) droplets. Absolute NPPA-AS1 levels
41 were initially presented as copies/ μ L cDNA based on the input amount of cDNA. Primers and
42 probe for NPPA-AS1 are listed in **Table 2**.

43 Statistical analysis

44 Significant differences among groups (>2) was determined by one-way ANOVA and

1 Holm-Sidak post-hoc test or two-way ANOVA and Holm-Sidak post-hoc test and Student's t-test
2 for differences between two groups. P< 0.05 was considered significant.

4 **References**

- 5 1. deAlmeida AC, van Oort RJ, Wehrens XH, Transverse aortic constriction in mice. *J Vis Exp.*
6 2010;(38):1729.
- 7 2. Viereck J, Kumarswamy R, Foinquinos A, Xiao K, Avramopoulos P, Kunz M, Dittrich M,
8 Maetzig T, Zimmer K, Remke J, Just A, Fendrich J, Scherf K, Bolesani E, Schambach A,
9 Weidemann F, Zweigerdt R, de Windt LJ, Engelhardt S, Dandekar T, Batkai S, Thum T. Long
10 noncoding rna chast promotes cardiac remodeling. *Sci Transl Med.* 2016;8:326ra22.
- 11 3. Liu Y, Wang Z, Xiao W, MicroRNA-26a protects against cardiac hypertrophy via inhibiting
12 GATA4 in rat model and cultured cardiomyocytes. *Mol Med Rep.* 2016;14(3):2860-6.
- 13 4. del Monte G, Casanova JC, Guadix JA, MacGrogan D, Burch JB, Pérez-Pomares JM, de la
14 Pompa JL. Differential notch signaling in the epicardium is required for cardiac inflow
15 development and coronary vessel morphogenesis. *Circ Res.* 2011;108:824-836.
- 16 5. Song J, Zhu Y, Li J, Liu J, Gao Y, Ha T, Que L, Liu L, Zhu G, Chen Q, Xu Y, Li C, Li Y.
17 Pellino1-mediated TGF- β 1 synthesis contributes to mechanical stress induced cardiac
18 fibroblast activation. *J Mol Cell Cardiol.* 2015;79:145-56.
- 19 6. Z. P. Huang, J. Chen, H. Y. Seok, Z. Zhang, M. Kataoka, X. Hu, D. Z. Wang, MicroRNA-22
20 regulates cardiac hypertrophy and remodeling in response to stress. *Circ Res.*
21 2013;112(9):1234-43.
- 22 7. T. Takaya, T. Kawamura, T. Morimoto, K. Ono, T. Kita, A. Shimatsu, K. Hasegawa,
23 Identification of EP300-targeted acetylated residues in GATA4 during hypertrophic responses
24 in cardiac myocytes. *J Biol Chem.* 2008;283(15):9828-35.
- 25 8. V. Tusher, R. Tibshirani, and G. Chu. Significance analysis of microarrays applied to the
26 ionizing radiation response. *Proc Natl Acad Sci USA.* 2001;98(9):5116-21.
- 27 9. J. D. Storey. A direct approach to false discovery rates. *J R STAT SOC B.* 2002;64:479-498.
- 28 10. G. Wu, J. Cai, Y. Han, J. Chen, Z. P. Huang, C. Chen, Y. Cai, H. Huang, Y. Yang, Y. Liu, Z. Xu,
29 D. He, X. Zhang, X. Hu, L. Pinello, D. Zhong, F. He, G. C. Yuan, D. Z. Wang, C. Zeng,
30 LincRNA-p21 regulates neointima formation, vascular smooth muscle cell proliferation,
31 apoptosis, and atherosclerosis by enhancing p53 activity. *Circulation.*
32 2014;130(17):1452-1465.
- 33 11. He A, Gu F, Hu Y, Ma Q, Ye LY, Akiyama JA, Visel A, Pennacchio LA, Pu WT. Dynamic
34 gata4 enhancers shape the chromatin landscape central to heart development and disease. *Nat*
35 *Commun.* 2014;5:4907.
- 36 12. Pei H, Wei L, Chiou HL, Jin Y, Ching S, Sylvia TN, Kevin KJ, Wei HX, Chieh
37 YL, Chien JL, Yi QX, Huanchieh C, Bin Z, Euan As, Daniel B, Peng
38 SC, Hueim SVC, Thomas Q, Ching PC. A long noncoding RNA protects the heart
39 from pathological hypertrophy. *Nature.* 2014; 514 (7520):102-6.